Topical Review

Fabrication methods and applications of microstructured gallium based liquid metal alloys

M A H Khondoker and D Sameoto

Department of Mechanical Engineering, University of Alberta, Edmonton, Alberta, T6G 2G8, Canada

E-mail: sameoto@ualberta.ca

CrossMark

Abstract

This review contains a comparative study of reported fabrication techniques of gallium based liquid metal alloys embedded in elastomers such as polydimethylsiloxane or other rubbers as well as the primary challenges associated with their use. The eutectic gallium–indium binary alloy (EGaIn) and gallium–indium–tin ternary alloy (galinstan) are the most common non-toxic liquid metals in use today. Due to their deformability, non-toxicity and superior electrical conductivity, these alloys have become very popular among researchers for flexible and reconfigurable electronics applications. All the available manufacturing techniques have been grouped into four major classes. Among them, casting by needle injection is the most widely used technique as it is capable of producing features as small as 150 nm width by high-pressure infiltration. One particular fabrication challenge with gallium based liquid metals is that an oxide skin is rapidly formed on the entire exposed surface. This oxide skin increases wettability on many surfaces, which is excellent for keeping patterned metal in position, but is a drawback in applications like reconfigurable circuits, where the position of liquid metal needs to be altered and controlled accurately. The major challenges involved in many applications of liquid metal alloys have also been discussed thoroughly in this article.

Keywords: liquid metals, eutectic alloys, stretchable electronics, EGaIn, gallinstan, manufacturing, microfluidics

(Some figures may appear in colour only in the online journal)

1. Introduction

3D structures of electrically conductive materials embedded in elastomers have great potential in a number of smart material applications, such as soft-matter sensors, actuators, flexible electronics, reconfigurable antennas and others. These applications have three main requirements; high flexibility, extraordinary stretchability and high electrical conductivity. While the flexibility of elastomers is well known and easy to achieve with materials like polydimethylsiloxane (PDMS), polyurethane rubbers and others, achieving high electrical conductivity in materials that can achieve strains of more than 100% (as is typical for elastomers) is extremely difficult. There are many reports where researchers have used a combination of inorganic and organic materials for flexible and/or stretchable electronic applications not requiring superior electrical conductivity, such as a stretchable form of single-crystal silicon in micro structures [1], transparent ZnO film and chalcogenides [2], polypyrrole conducting polymers [3],

polypyrrole-poly (ethylene-co-vinyl acetate) composites [4], PDMS—CNT/graphene conducting polymers [5–9], silver-nanowire (AgNW)—polyacrylate composite [10], PDMS—Ag conducting composites [11, 12], cellulose—indium tin oxide (ITO) electrodes [13], polyurethane/PEDOT:PSS conductive composite [14] etc. Inkjet printing technology [15–17] has also been utilized for flexible electronics applications but still these applications have limited stretchability and relatively lower electrical conductivity compared to that of metals. In general, the introduction of electrically conducting fillers to elastomers is reasonably simple and can produce stretchable conductors but they are multiple orders of magnitude less conductive than metals and frequently strain sensitive in their conductivity, which limits their use in applications requiring high currents, or very high frequencies. While flexibility is very important for thin-film electronics and their applications, bending flexibility does not necessarily mean that high elongations are possible, and stretchable electronic conductors may be more attractive in applications like artificial muscles [18], soft robotics [19] and tactile sensors [20, 21].

Many examples exist where rigid, high conductivity components are integrated with flexible and stretchable materials for flexible or stretchable electronics. Because of its superior electrical conductivity, copper (Cu) might be a top choice electrically but its hardness makes it unable to withstand repeated bending and it will experience plastic deformation with a strain of approximately 2% [22]. There are a number of reported methods and materials for stretchable electronics [23, 24]. Among them, metallic wires with thin coil shapes encased in elastomer materials have become a very popular method to overcome this particular challenge in flexible and stretchable electronics. These use specialized folded geometries of electrodes to permit stretching and compression without exceeding local elastic limits. Among them, micro-sized helical wires [25], horseshoe like forms of gold [26] or copper [27], laser ablated copper foil in silicone [28], gold micro-wires with tortuosity [29], copper film by electroless deposition [30], meander-shaped nickel-gold layer in PDMS [31], and metal ion implanted elastomers [32], showed some feasibility to be used in flexible and/or stretchable electronics applications due to their high conductivity. Furthermore, thin layers of copper, chrome or gold [33–35] and thermochromic liquid crystals [36] have also been utilized with elastomers (e.g. PDMS) in epidermal electronics applications [37]. Rahimi *et al* showed sewing enabled meander wire systems embedded in elastomer [38] and Wang *et al* used pre-strained elastomers covered with metal that then buckles as an alternative to meander electrodes [39]. Unfortunately, these devices are still ultimately limited by inherent rigidity of the metal layers and require unnecessary design constraints by the increasing complexity of fabrication. At higher bending or stretching, they start begin to crack at the micro level, and there is also the danger of possible delamination between the elastomers and the rigid materials contained within that may occur at extreme strains. While many of the thin-film electronics reported for flexible circuity make use of clever designs of electrodes and very thin

materials to ensure they conform to skin or other deformable surfaces, the applications only require very small currents, and the thin film strategies may not be scalable to smart materials where significant current may eventually be used.

Due to the challenges with traditional metallic micro-structures and organic/inorganic thin film structures, researchers began looking for materials with higher electrical conductivity as well as better flexibility. Liquid metals at room temperature are the best suited conductive materials in this field because they enable conductive paths embedded in elastomers to be stretched or bent repeatedly without significant loss in their performance. As the best known liquid metal, Mercury (Hg) has been used in different flexible electronics applications [40–42]. Unfortunately it has a serious disadvantage in that it is highly toxic [43, 44]. Other elements which are liquid near room temperature also have their own drawbacks; caesium (Cs) may be radioactive and is violently reactive, and rubidium (Rb) has violent reactive nature. Pure gallium is liquid at approximately 30 °C, but this is too high to remain liquid in most room temperature applications (although it is perhaps compatible if in close contact with body heat). Therefore, these pure metallic elements are also limited in their use in the flexible electronics and bio applications.

Over the last decade gallium based liquid alloys have gained increasing popularity as materials best suited for fulfilling both the requirements for high electrical conductivity and extreme flexibility. As a liquid metal at room temperature, the eutectic alloy of 75.5% gallium (Ga) and 24.5% indium (In), EGaIn has recently attracted considerable interest from many researchers. It can be attributed to the advantageous properties of this alloy in embedded elastomers. An alternative room temperature gallium alloy, galinstan is composed of gallium, indium and tin with varying compositions. Since the melting point of galinstan is dependent on the ratio of three components, there is no generic value of melting point. But the typical galinstan (68.5% Ga, 21.5% In and 10% Sn) has a reported melting point of −19 °C, whereas EGaIn has melting point of 15.5 °C [45]. Therefore, these non-toxic alloys [46, 47] will remain liquid at most comfortable temperatures that may be found indoors and possess virtually no vapor pressure [42]. In addition, they have quite low viscosity in their liquid phase and a relatively high electrical conductivity (approximately 1/16th that of copper [48]). In their liquid state, these alloys are electrically more conductive than in their solid state [49]. If the oxygen level in the ambient atmosphere is above 1 ppm [42] liquid gallium alloys start oxidizing and form a thin passivation oxide layer (Ga_2O_3 and Ga_2O) on their surface [50]. The thickness of the electrically resistive [51] oxide skin was found to be approximately 0.7 nm in x-ray diffraction tests under vacuum conditions [52], but it is much thicker (∼1–3 nm) in laboratory conditions [50, 53–56]. This oxide layer acts as a skin and can decrease the effective surface tension of the liquid metal in electrochemical reactions [57], or if the oxide is breached. As a result, the liquid metal tends to wet other surfaces (unlike mercury), which helps to maintain non-spherical metal structure even in microchannels [55, 58]. The wetting caused

by this oxide skin can also lead to the tendency to stick to any solid surface [50] even if undesired, so this particular feature of gallium based alloys can be a benefit or drawback depending on the application. Doudrick *et al* demonstrated that galinstan adhesion occurs in two steps [59]. First, the oxide skin does not rupture when galinstan makes contact with substrate surface. The nanoscale topology of the oxide skin allows only minimal adhesion between galinstan and substrate surface, regardless of its surface energy. In the second step, oxide skin ruptures and now old oxide skin—substrate surface, bare galinstan—substrate surface and new oxide skin—substrate surface adhesions occur. It also was found that the adhesion between the new oxide skin and the substrate surface dominates the total adhesion in this second step.

The ability of these alloys to flow through the channels on demand permits them to be designed as 'reconfigurable' as the dimensions of the channels can be changed if they are made of elastomers, and other fluid handling mechanisms, such as valves and pumps [60–64] may be used to control specific location and electrical connections of these liquid metals. Other than acting as the primary material, liquid metal can also be used just to exploit its fluidic nature. For example, Tang *et al* demonstrated liquid metal enabled pump, where a droplet of liquid metal induces flow of a range of liquids without mechanical moving parts by means of electrowetting/deelectrowetting at the metal surface [65], and Boley and Gui proposed a liquid metal based electroosmotic flow pump [66]. Kim *et al* reported real-time dynamically reconfigurable photomask, where on-demand injection and withdrawal of liquid metal in microchannel was utilized to change the patterns of photomask [67]. Other benefits of using EGaIn/galinstan for smart materials include their high thermal conductivity, and low vapor pressure (which ensures negligible evaporation and mass loss). Therefore, these gallium based liquid metals have been extensively utilized in flexible, stretchable electronics applications and can be an alternative to wavy and highly stretchable wearable electronics [23, 68]. Because they are liquid at room temperature, the majority of applications using liquid gallium alloys have them contained inside some solid channel system (e.g. tunable frequency selective surfaces (FSS) [69], micro-variable inductor [70] etc), but the applications of these liquid metals are not limited to only embedded applications. For instance, in some reported work [71], liquid gallium alloy has been successfully used in injection of femto-litre sized samples into cells. Ladd *et al* successfully printed freestanding columns and spheres of EGaIn [72]. Other than electronics applications, liquid metals also have potential to be used in thermal applications [73–75] as a heat sink or conductor to manage temperatures. Other than using as main functional element, Kim *et al* used liquid metal as secondary element [76] which was a liquid metal via connecting stretchable patterned gold layers. For comparison purposes, the properties of functional materials used in flexible electronics applications have been summarized in the following table 1. From this point on, in this review, 'liquid metal' will refer to the gallium based alloys EGaIn and galinstan. This report is intended to present the comparative

study on the fabrication processes of two and three dimensional micro-structures of liquid metals using different techniques reported already.

2. Fabrication processes of liquid metal micro-structure

There are a number of reported fabrication processes of liquid metal to form embedded micro-structures. These techniques can be grouped under four major classes such as masked deposition, imprinting, direct patterning and casting. Among these broad categories, masked deposition techniques result in relatively large feature sizes [84], whereas fabrication processes by casting are the most popular technique which produces smallest reported minimum feature size of approximately 150 nm [85]. Many of these techniques classified under these four main groups have been summarized in table 2.

The broad category of techniques listed in the following section is organized roughly by the increasing quality and complexity of designs feasible with each technique, although there are large variations in those properties between individual reports.

2.1. Masked deposition

There are a number of masked deposition techniques, which use different methods to selectively deposit liquid metal alloys. These techniques have been discussed below.

2.1.1. Using a stencil. Embedded structures of liquid metal can be created using 3D printed masks [86] or stencils [84, 87] to pattern the metal followed by encapsulation steps. In the case of work presented in [86], a mask was placed in contact with a silicone (Ecoflex 0050) which could conform to mask roughness and contain EGaIn which was dispensed manually. To remove the mask cleanly, the EGaIn was cooled below the freezing point to solidify it, and then another layer of silicone (Ecoflex 0010) was spin coated on top while the EGaIn was still frozen, and then the silicone was cured at elevated temperatures. Repeating this process allowed multiple layers of independent liquid metal to be embedded within a flexible elastomer for the ultimate use as a capacitive sensor to detect shear and pressure. In another stencil based process as shown in the figure 1, a copper stencil is first placed on the partially cured PDMS substrate material. Then, excess amount of liquid metal is poured on the stencil. To ensure the uniform thickness of liquid metal in the openings of the stencil, a liquid alloy wetted roller can be rolled repeatedly [84]. This roller also helps to remove excess alloy material. Finally, the stencil is removed and the patterned structure of liquid alloy remains on the substrate. After that, depending on the application, a sealing elastomer layer can be applied by successive spinning and curing process. Just as in [86], the stencil works well because the underlying PDMS can conform to make a good seal, while having low inherent adhesion so that the stencil may be removed without

Table 1. Properties of selected liquid metals, low melting pure metals and other conductive materials.

Functional materials/ composites	Melting point T_m (°C)	Viscosity ν (cSt)	Surface tension γ (mN m^{-1})	Conductivity σ (10^7 S m^{-1})	Major drawbacks
EGaIn	15.5 [45]	0.32 [55]	624[a] [77]	0.34 [58, 78]	—
Galinstan	−19 [79]	0.37 [79]	535[a] [42]	0.38 [79]	—
Ga	29.8	—	—	0.37	Solid
Hg	−39 [79]	0.11 [79]	428 [80]	0.10 [79]	Toxic
Cs	28.5	—	—	0.50	Violently reactive
Rb	39.3	—	—	0.83	Violently reactive
Cu	1085	—	—	5.97 [46]	Low flexibility
Ag	961.8	—	—	6.30 [46]	Low flexibility
Ni	1455	—	—	1.43 [46]	Low flexibility
ZnO film	1975 [81]	—	—	7.55×10^{-17} [82]	Low conductivity
Polypyrrole-poly (ethylene-co-vinyl acetate)	—	—	—	$5–7 \times 10^{-5}$ [4]	Low conductivity
Polypyrrole conducting polymer	—	—	—	9.7×10^{-4} [83]	Low conductivity

[a] Oxidized value.

difficulty. The smallest feature reported in this process was 200 μm and minimum spacing was 100 μm, although whether this was a limitation of the stencil or the deposition process was unclear.

The stencil technique is relatively simple, reliable and can have high throughput. But it's suitable for only relatively large features and a limited class of geometries. In particular, the surface of the liquid metal after deposition is frequently quite rough and not very uniform in thickness [84]. The stencils may also be more challenging to use multiple times without cleaning, as increased layers of oxidized gallium can build up and be transferred to unwanted locations. One primary attraction to the stencil process is that isolated areas of liquid metal can be readily patterned and in theory quite large areas can be patterned in a single step.

Very recently, a new technique, atomization patterning, has been reported to produce liquid metal structures [120]. It sprays atomized liquid metal with nitrogen as a carrier gas onto a semi-cured PDMS surface with a tape transferred adhesive mask. This is also masked deposition but unlike the previously described techniques, it uses a spray to apply liquid metal alloy. This method results in smooth line edges compared to other masked deposition techniques.

2.1.2. Selective wetting.
This masked deposition technique uses a sacrificial layer instead of using a stencil to wet the substrate selectively by liquid metal (galinstan in this case). Kramer *et al* [88] has described the whole process in detail as shown in figure 2. First, a polytetrafluoroethylene (PTFE) particle-filled photoresist, tin foil and PDMS are layered on a glass slide. Then, PTFE and tin foil are patterned using photo-lithography. A thin layer of PAA is applied by spin coating and it spontaneously dewets from the super-hydrophobic PTFE/photoresist. Now, the whole surface is sputtered with indium, and then flooded with acetone to lift-off indium on the photoresist. When the liquid metal is applied on the patterned tin foil, it reactively wets it while not adhering to the photoresist. A thin-film applicator is used to wipe the excess

amount of liquid metal off the surface. Finally, the sputtered PAA layer is removed by rinsing in water and a sealing layer of elastomer is applied. At this stage, the gallium is then frozen (below −19 °C) and encapsulated with another layer of curable silicone.

This masked deposition technique usually produces rough edges and is appropriate only for a limited class of geometries. The use of spontaneously wetting and dewetting areas is a novel approach, but ultimately has similar capabilities and advantages in terms of patterning features as the stencil systems described earlier. As implied in figure 2, the features will still have a rounded cross-section due to the surface tension effects on the liquid metal. The requirement of using photolithography and sputtering in this approach would be disadvantageous from a processing point of view but the uses of microstructured surfaces to aid in repelling or enhancing bonding may still be valuable in future variations.

2.2. Imprinting

Imprint processing can be a conceptually very simple method to produce patterns using liquid metals. Variations on this technique include dipping a structured stamp into liquid metal and transferring it to another surface, embossing a liquid metal film and producing separate structures by squeezing out metal, or by transferring from a single liquid metal film into recesses on a structured surface.

2.2.1. Printing in recesses.
This imprinting process using a mold is a very simple technique to pattern liquid metal and closely resembles a portion of the gravure or roll-to-roll (R2R) printing process [121, 122]. As reported by Gozen *et al* [89], a thin layer of liquid metal is applied on a flat surface. Separately, a PDMS mold with desired topographical features is produced. Then, the PDMS mold is pressed against the liquid metal layer which then fills in the recesses. Due to the stickiness property of gallium-oxide layer, a very small amount of liquid metal adheres to the elevated walls of the

Table 2. Reported fabrication techniques of liquid metal structures embedded in elastomers.

Fabrication	Techniques	Minimum reported feature size	Advantages	Disadvantages	Devices fabricated
Masked deposition	Using a stencil	Line width = 200 μm Spacing = 100 μm [84]	Relatively simple; Reliable; High throughput;	Large feature size; Limited class of geometries; Rough edge;	Shear and pressure sensor [86]; RFID antenna [84]; Galinstan heater [87];
	Selective wetting	Line width = 100 μm Spacing = 25 μm [88]	Relatively simple; Reliable; High throughput;	Rough edge; Limited class of geometries;	Patterned structures [88];
Imprinting	Printing in recesses	Line width = 2 μm Spacing = 1 μm [89]	Very small feature size;	Residue on outside of channels; Rough edge;	Coplanar capacitor [89];
	Printing using stamp	Line width = 0.75 mm Spacing = 1 mm [87]	Relatively simple; Can be performed manually;	Large feature size; Uneven wetting;	Planar circuit [87];
	Screen printing	Line width = 40 μm [90]	Micro-scale droplets	Requires pressure control;	[90];
	Micro-contact printing	Line width = 340 μm [87]	Any arbitrary planar geometry; Requires limited manual labor;	Requires motion control; Needs repeated contacts; Rough edge;	Comb capacitor [87];
Direct patterning	Pressure driven 2D structure	Line width = 45 μm [91]	Any arbitrary 2D structure;	Relatively complex technique;	Interconnect [91]; Directly written traces [92]; Printed circuit and pattern [93];
	Pressure driven 3D structure	Line width = 150 μm [72]	3D free-standing structures;	Need good control on injecting;	Free standing 3D structures [72];
	Dielectro-phoresis based 3D structure	Width = 80 μm Spacing = 40 μm [94]	Finer 3D features with relatively smooth surface; Possible with wide range of designs.	Requires chromium/gold pads deposited previously; Requires power supply	Microelectrodes and microfins [94];
	Laser patterning	Line width = 100 μm [95]	Any arbitrary 2D structure;	Higher wastage of liquid metal;	Patterned LED circuit [95];
Casting	Needle injection	Line width = 150 nm [85]	Fast and reliable; Relatively simple; 3D embedded structures; Better resolution; Smoother sidewalls;	Limited class of geometries; Requires two terminals; Air trapping is common;	Stretchable interconnect [96]; Cube antenna [97]; Tunable antenna [98]; Microelectrodes [99]; Planar inverted cone antenna [100]; GaIn nanowires [85]; Capacitors and inductors [101, 102]; Electrostatic actuator [103]; Radiofrequency antennas [104]; RF radiation sensor [105]; Diodes [106]; Memristor [107]; Pressure sensor [108]; Soft artificial skin [109, 110]; Force sensor skin [111]; Wearable tactile keypad [112]; Strain sensor [113]; Curvature sensor [114, 115]; Ultrastretchable conductors [116, 117]; Loop antenna [118];

7

Table 2. (Continued.)

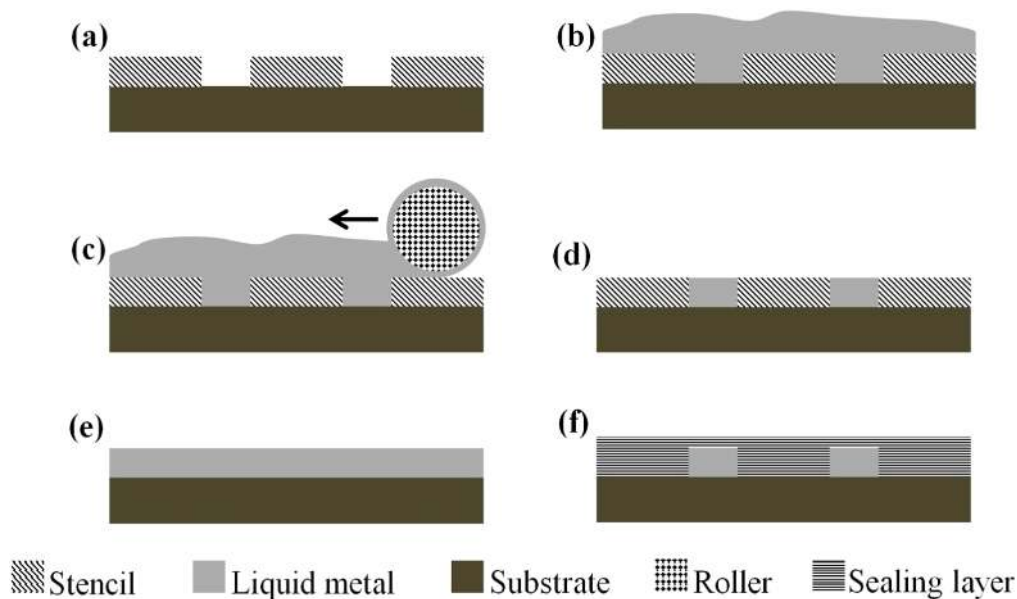| Fabrication	Techniques	Minimum reported feature size	Advantages	Disadvantages	Devices fabricated
Casting	Vacuum assisted infiltration	Line width = 250 μm [119]	No need of two terminals; Deep features; Structures with different height;	Needs repeated process;	Comb capacitor [97]; Planar circuit [119];

Figure 1. Masked deposition using stencil. (a) stencil placed on substrate, (b) excess amount of liquid metal is applied, (c) use of roller (d) uniform thickness of liquid metal in the openings of stencil, (e) patterned alloy after removal of stencil and (f) finally, application of sealing elastomer layer (inspired by [84] with permission of The Royal Society of Chemistry and with permission from [87] Copyright 2013 American Chemical Society).

recesses of the mold, but the recesses can remain filled. In this way, even after the mold is removed, liquid metal alloy remains in the patterned structure. Finally, a sealing layer can be applied to embed the structure. This method is illustrated in figure 3.

Using this technique, Gozen et al fabricated a coplanar capacitor having only 2 μm thick lines with 1 μm spacing—several orders of magnitude smaller than the features reported with stencil processes. Unfortunately, the liquid metal is not completely non-wetting on the top PDMS surface and a reported problem with this method is that a residual layer of liquid metal is observed on the top of the walls outside of the channels. This technique could be potentially improved with the addition of super-hydrophobic structuring of the top surface to get more dewetting, similar to the technique in [88], while not diminishing the subsequent bondability with silicone.

2.2.2. Printing using stamps. This technique is very similar to imprinting with a mold but uses the raised surfaces of a stamp to transfer areas of liquid metal onto another surface. It starts with the preparation of a PDMS stamp with topographical features by casting. Tabatabai et al [87] used a 3D printed mold to cast the PDMS stamp. Using a paint brush, the raised surfaces of the stamp are inked with liquid metal alloy. Then, the stamp is pressed on the substrate and the liquid metal is transferred. A frame is placed encompassing the patterned structure and using successive spin coating and curing, a sealing layer of elastomer is applied on top of the patterned liquid structures. To reduce or eliminate displacement of the liquid patterned structure during spin coating, it might be helpful to freeze the liquid metal structure before spinning and therefore EGaIn is a better choice than galinstan in this regard. The steps involving

stamp lithography are shown in the figure 4. Tape transfer printing [123] proposed by Jeong et al also uses the same principles to fabricate stretchable RF electronics.

Tabatabai et al prepared a Sylgard 184 PDMS stamp with features protruding 2 mm from the stamp base and printed features with as small as 0.75 mm wide with 1 mm spacing using this process onto another silicone (Ecoflex 0030). This is very simple process, and can be done manually, but it is limited to relatively large features. Another problem arises because of uneven wetting of the stamp and target surface, which may result in non-uniform thickness or missing areas of the liquid metal features. Of the three distinct methods reported by Tabatabai et al (inkjet printing, micro contact printing and stamp lithography) this stamp lithography was determined to be the least reliable.

2.2.3. Screen printing. As described by *Sen and Kim* [124], the work by Truong et al [90] applies a version of silk-screen printing with a screen prepared by KOH bulk etching of silicon to produce microscale openings. When a print-head containing a reservoir of liquid metal is pressurized, the liquid metal bulges out through the openings of the screen and is deposited on surface that had been pre-patterned with gold to enhance the wetting of liquid metal. After that, as soon as the screen is withdrawn, the wetting pad forces liquid metal to form droplets and adhere on it. The schematic of this process is shown in figure 5. The openings of the screen have a width distribution of 40–70 μm. This process requires a level of expertise to apply controlled pressure on print head, which influences the amount of material transferred and the quality of the feature.

2.2.4. Micro-contact printing. Micro-contact printing (μCP) of liquid metal alloy was first reported by Tabatabai et al [87].
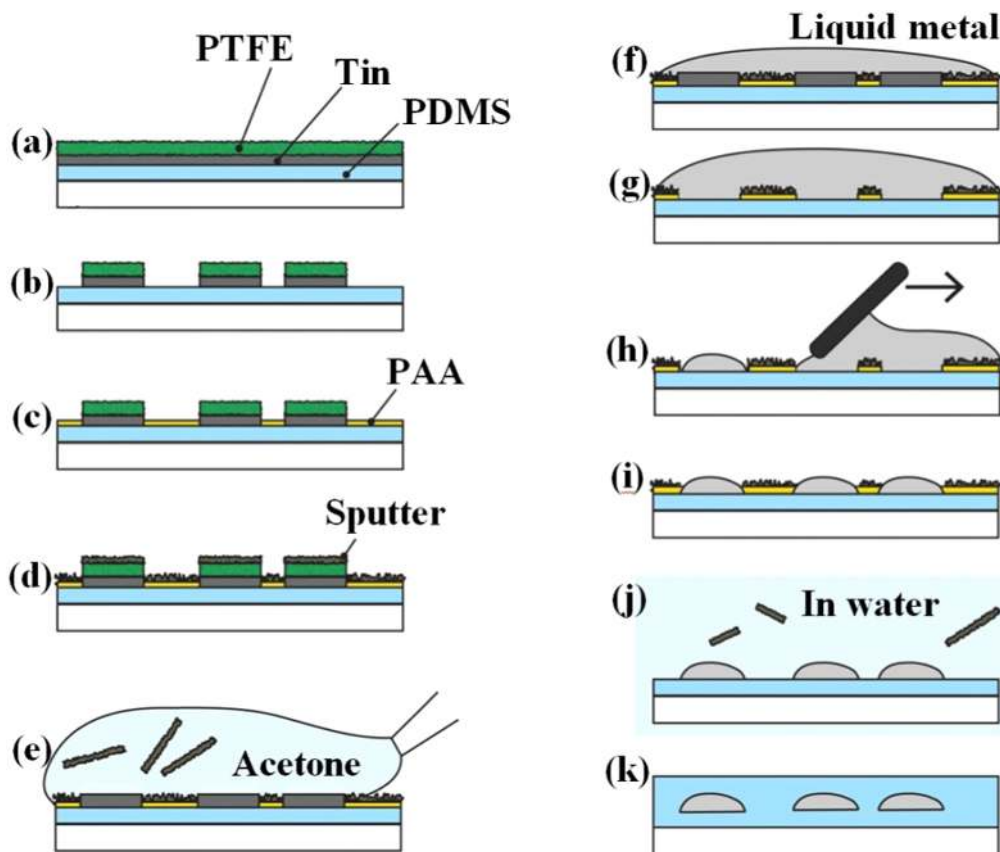
Figure 2. The masked deposition through selective wetting (adapted from [88]. Copyright WILEY 2013 reprinted with permission).
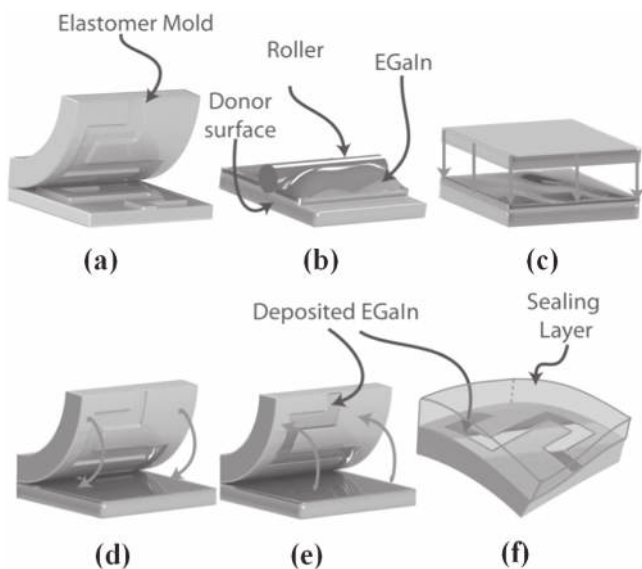

Figure 3. Imprinting using PDMS mold. (a) PDMS mold with desired topographical feature is prepared, (b) a thin layer of liquid metal alloy is applied on a flat surface, (c) flattening and removal of excess liquid metal, (d) the PDMS mold is pressed against liquid metal, (e) liquid metal adheres to the walls of recesses of the mold and (f) application of sealing elastomer layer (adapted from [89]. Copyright WILEY 2014 reprinted with permission).

In this imprinting technique, a hemispherical PDMS tip is used as the nozzle. This nozzle is mounted on the print head, which is controllable along *x*-, *y*- and *z*-directions by means of a user defined Matlab program. When the tip is dipped into liquid metal, the nozzle collects a bead of liquid metal. Then, the nozzle is moved to contact the substrate to transfer a small droplet of liquid metal at the desired position. This imprinting technique mainly depends on the adhesion of liquid metal to the elastomer. Tabatabai *et al* measured the diameter of these droplets as 340 μm. If the successive droplets have spacing less than their diameter (340 μm), these droplets coalesce to form a continuous line. In this manner, a desired pattern of liquid metal is printed on the PDMS substrate. Finally, when solidified, this pattern can be embedded by a sealing layer of PDMS. This technique is illustrated in the figure 6.

Since the motion of the print head is controlled by a separate motorized 3-axis Cartesian system, any arbitrary planar geometry is possible in this method subject to the minimum dimension restrictions caused by the droplet size. It also requires minimal manual labor compared to many other deposition techniques reported in the literature. One major disadvantage of this technique is the need of repeated contacts rather than a continuous printing.
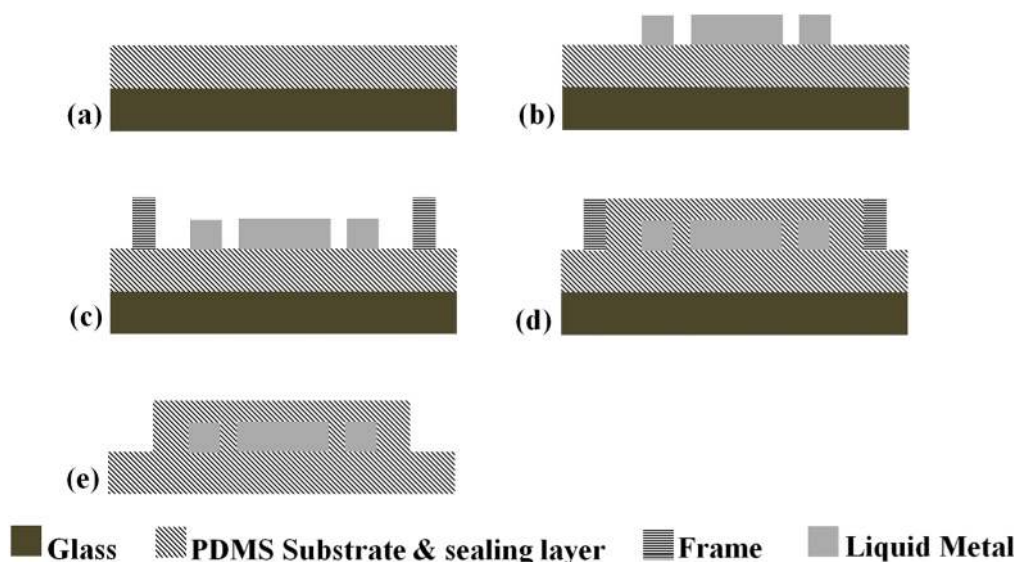
Figure 4. The steps involved in stamp lithography. (a) Preparation of base PDMS layer on glass substrate, (b) patterned liquid metal after imprinting using wetted stamp, (c) placement of a frame encompassing the structure, (d) application of sealing layer of PDMS and (e) removal of glass plate and frame gives the embedded structure of liquid metal in PDMS (inspired by [87]).
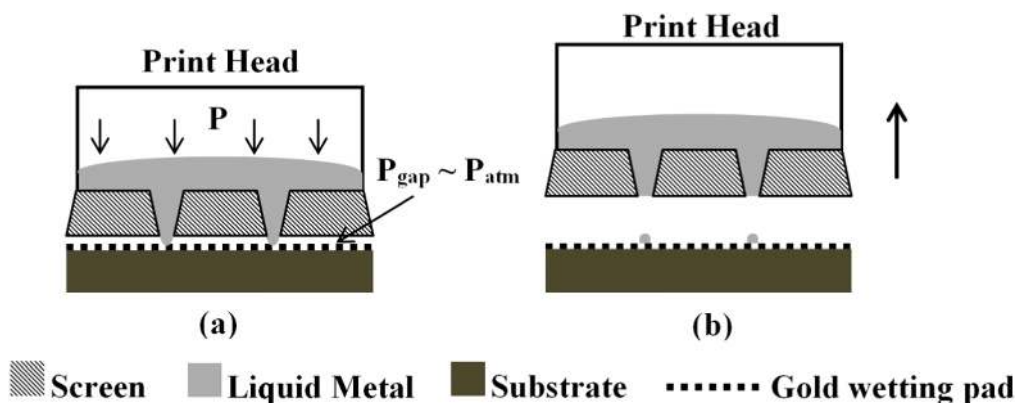

Figure 5. The screen printing technology. (a) The print head with screen is pressed on the gold wetting pad and (b) the droplets of liquid metal are bulged out to pattern on substrate (inspired by [90]).

2.3. Direct patterning

In this section, the techniques to directly pattern 2D and 3D structures of liquid metal alloys have been summarized.

2.3.1. Pressure driven 2D structure.
In these pressure driven techniques, a simple roller-ball pen and brush pen were used to directly write conductive tracks of liquid metal ink on different substrates with relatively low resolution by Zheng *et al* [125] and Gao *et al* [126, 127], respectively. Later on, high resolution electronic circuits of liquid metal were successfully printed by Yang *et al* [128] and Zheng *et al* [93] using a customized computer-controlled liquid metal printer. The printing head developed by Zheng *et al* comprises a tiny rolling sphere inside the dispensing nozzle. Enforced pressure of liquid metal and the rolling sphere contribute to uniformly transfer liquid metal to the substrate, whereas the oxidation of liquid metal ensures the adhesion to the printing substrate. After printing the desired circuit on flexible PVC film, the circuit can be transferred to a PDMS

film and subsequently sealed with another layer of PDMS to get the embedded structure described in [129]. In a separate work, Zheng *et al* also developed a brush-like porous needle pen and customized commercial rubber dispenser to fabricate printed-circuits-on-paper flexible electronics [130]. In brief, the customized printer system was equipped with two syringes preloaded with liquid metal and room temperature vulcanization (RTV) silicone rubber. First, conductive patterns were printed on paper using one syringe, and then RTV silicone rubber was overprinted using another syringe to get three dimensional hybrid electro-mechanical devices on paper.

In an alternative direct printing method, Kim *et al* used a custom print head with an orifice to jet liquid metal onto the desired substrate [91]. This custom print head has HCl-impregnated flattened paper near the orifice to reduce oxidation and ease jetting. Another group of researchers, Boley *et al* used direct writing method to pattern a liquid metal structure on a substrate [92]. In this method, a
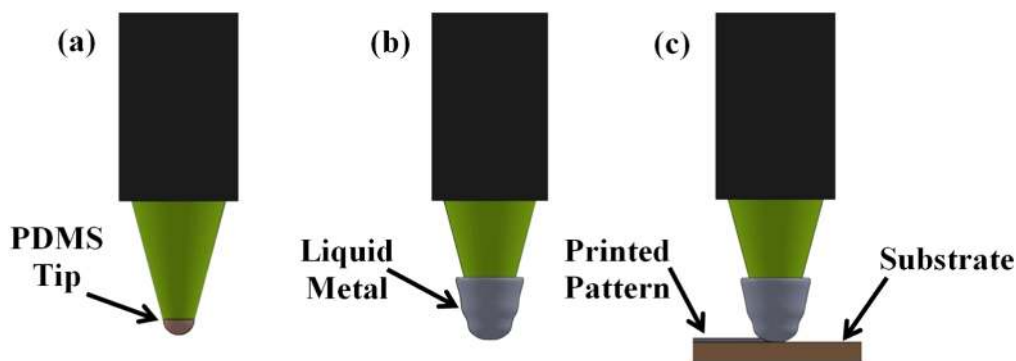
Figure 6. The μCP of liquid metal inspired by [87]. (a) Printing head with hemispherical PDMS tip, (b) the nozzle is wetted in liquid metal and (c) The wetted nozzle makes lines comprising sequential droplets.
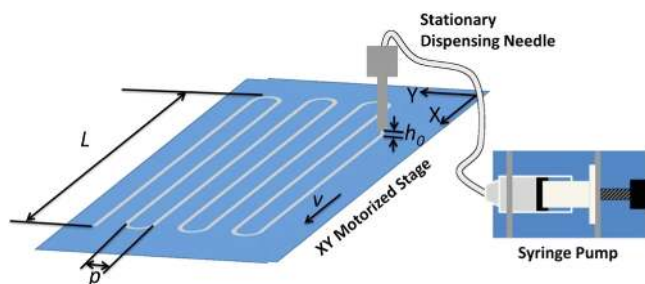

Figure 7. The schematic of direct writing with dispensing needle adapted from [92]. Copyright WILEY 2014 reprinted with permission.

stationary syringe needle was used to dispense liquid metal onto a movable substrate by using a syringe pump. Both Boley *et al* and Kim *et al* have used a syringe pump to feed the liquid metal through the nozzle. The detailed procedure to fabricate the custom print head by Kim *et al* can be found in literature [91]. The writing system reported by Boley *et al* is schematically illustrated in the figure 7. Boley *et al* observed that for stable writing, the ratio of standoff distance (h_0) above the substrate and the inner diameter (ID) of the writing nozzle must not exceed a critical value ($h_0/\text{ID} < \approx 0.21$ for stable writing) [92]. No failures were observed at very close distances, but there would be a possibility for the tip to contact and drag accidentally if h_0 was set too low.

Inkjet printing of liquid metals is another fabrication technique, which results in the same pressure driven 2D structure but has different post-processing requirements to ensure proper coalescence of jetted droplets. Compared to the direct writing by Boley *et al*, inkjet printing has more size restrictions. For the inkjet printing system reported by Kim *et al*, the flow rate of liquid metal through the nozzle determines the size of the jetting droplets. For nozzles made of pure PDMS, flow rates below $0.5\,\text{ml}\,\text{min}^{-1}$ could not overcome the surface tension caused by the native oxide to jet droplets and a large droplet at the outlet can continuously increase in volume. For the HCl-impregnated tip, the pinched off droplet diameters at this flow rate were approximately $500\,\mu$m. At higher flow rates, faster jetting produces smaller droplets (as small as $1\,\mu$m diameter) [91]. These techniques are comparable with traditional inkjet printing. The suitability

of inkjet printing technique to any ink or fluid mainly depends on how the jet undergoes breakup to form droplets, which is governed by the fluid properties i.e. viscous, inertial and surface tension forces. The fluidic properties of the liquid metal alloys do not favor its use in inkjet printing techniques without modifying those properties. On top of that, the oxide skin formed on to the liquid metal surfaces also impedes the droplet formation. For instance, Guangyong *et al* used HCL vapor to consistently remove oxide skin from liquid metal and successfully utilized in inkjet printing system without modifying the fluidic properties itself [131]. On the other hand, Boley *et al* have proved that if the dispersion of mechanically sinterable EGaIn nanoparticles is used, inkjet printing is a means for liquid metal devices like arrays of strain gauge with intricate wiring and contact pads [132]. Briefly, the dispersion of thiol-capped EGaIn nanoparticles (180–600 nm) were fabricated using multiple sonication stages of bulk liquid metal and ethanol/thiol solutions.

The minimum reported feature size from 2D direct patterning is $45\,\mu$m [91]. Though the main advantage of this technique is the possibility of producing any arbitrary 2D structure the major drawback is the requirement of a relatively complicated support system.

2.3.2. Pressure driven 3D structure. Ladd *et al* reported direct-write patterning methods to fabricate free standing liquid metal structures, wires, fibers, arrays of droplets and array of in-plane free standing lines [72]. A stationary syringe needle is used to extrude the liquid metal onto a movable, controlled stage and a syringe pump is used to apply appropriate pressure on the syringe.

To form the wires (figure 8(a)), a modest gauge pressure (<5 kPa) is applied on the syringe. As a result, a bead of liquid metal is built-up at the tip of the needle. If the metal contacts the substrate and the syringe is taken away slowly with constant pressure, a wire forms and elongates because of the tensile force generated due to the oxide layer. Wire forming is terminated by applying a vacuum on the syringe. By this method, a wire 1 cm long and $30\,\mu$m wide has been fabricated successfully.

Secondly, fibers (figure 8(b)) are produced by quickly expelling the liquid metal from the syringe using a burst
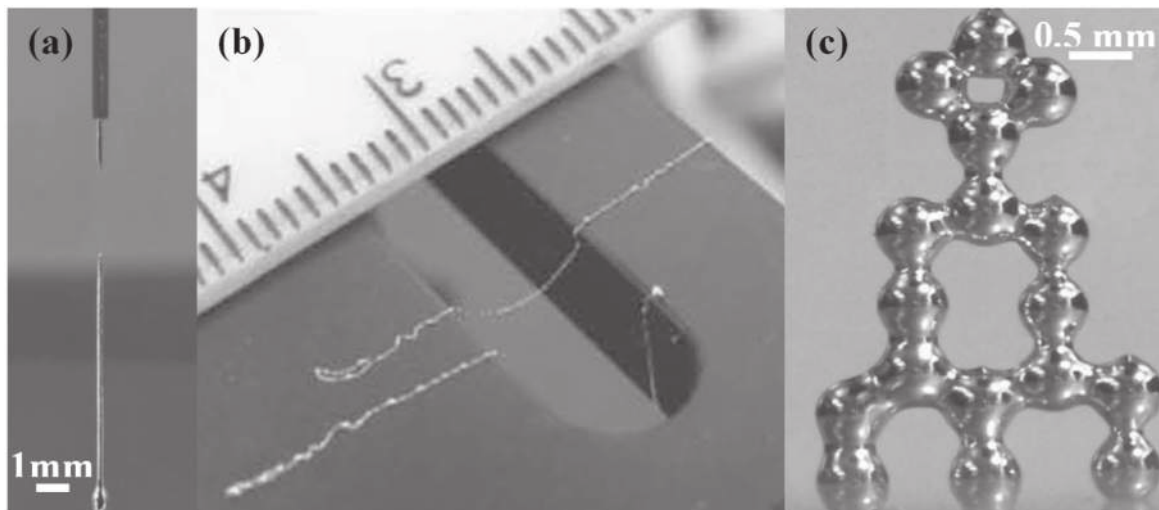
Figure 8. (a) Formation of free standing wire, (b) The suspended fibers using short burst pressure and (c) stacking the liquid metal droplets (adapted from [72]. Copyright WILEY 2013 reprinted with permission.).

pressure (~60 kPa). The stack of droplets shown in the figure 8(c) is fabricated by forming droplets using short burst pressure (20–60 kPa for 1–2 ms). The syringe needle carries the droplet until it touches the previous droplet. The droplets contact each other without coalescing into one bigger droplet.

2.3.3. Dielectropheresis based 3D structure.

Tang *et al* [94] introduced a novel technique to create 3D microstructures of liquid metal using dielectropheresis (DEP). The process starts from producing microdroplets (0.1–0.35 μm) of galinstan in deionized (DI) water with the help of ultra-sonication. In the second step, the microdroplet suspension was applied to a DEP platform having pairs of planar chromium/gold microelectrode pads with a diameter of 80 μm and a similar microelectrode island between each pairs of pads. The gap between these microelectrodes was only 40 μm. The electrically conductive liquid metal droplets were immobilized between the microelectrode pads when a sinusoidal signal (15 V, 20 MHz) was applied. This immobilization was caused mainly by the DEP force. Finally, NaOH solution was used to partially remove the oxide skin formed on microdroplets letting them to amalgamate on gold microelectrode pads. Then, a high flow is used to wash out the unmerged droplets, which then results in formation of 3D microelectrodes of liquid metal with a spherical cap as shown in the figure 9.

2.3.4. Laser patterning.

Direct patterning of liquid metal electrodes by using laser cutters was reported by Lu *et al* [95]. In this method, a commercial CO$_2$ laser cutter (VLS 3.50, 30 W) was used to remove liquid metal in a subtractive manner. As shown in figure 10, the process starts by encasing a thin layer of liquid metal between two layers of PDMS. The top layer of PDMS is cast and cured on top of the EGaIn to contain it, helps in initial removal of material by highly absorbing the laser light, and protects the EGaIn layer from excessive oxidation and debris contamination during the laser

cutting process. When the CO$_2$ laser is applied at a desired location, the energy from the laser vaporizes the top and bottom PDMS layers. The higher vapor pressure of vaporized PDMS punctures the liquid film and escapes, which results in a patterned planar structure of liquid metal. The technique uses the native Ga$_2$O$_3$ layer as an advantage, as the oxide is able to stabilize the EGaIn in its displaced position and permit features approaching 100 μm to be produced rapidly. Once the metallic features are patterned, a new layer of PDMS is cast on the structure to produce the fully encased electrodes. Using this technique and electrically conductive silicone composite materials, soft matter sensors for pressure measurements, and a flexible LED circuit were successfully demonstrated.

2.4. Casting

In these processes, the liquid metal alloys are filled into a mold with patterned cavity by means of different techniques and allowed to solidify by freezing, when required.

2.4.1. Needle injection.

Injection casting is the most widely used method to pattern 2D and/or 3D structures of liquid metal. Unlike all the previous techniques listed for direct printing, imprinting and stenciling, the use of injection permits much higher degree of control over the electrode dimensions, and cross-section. This advantage is balanced by the more complex processes necessary to produce the sealed channels in the first place, and the requirement for all features to be connected for a given injection step, which is a major drawback for more complex circuitry. Researchers have used the injection method in great variety of applications ranging from flexible electronics to soft artificial skin [85, 96–101, 103–115, 133]. In one particular implementation of the injection process, a flat glass plate is placed against a PDMS mold produced by casting or any other means. For example, White *et al* [133] used a rod-coating technique first to prepare elastomer films and then laser ablation to fabricate micro-
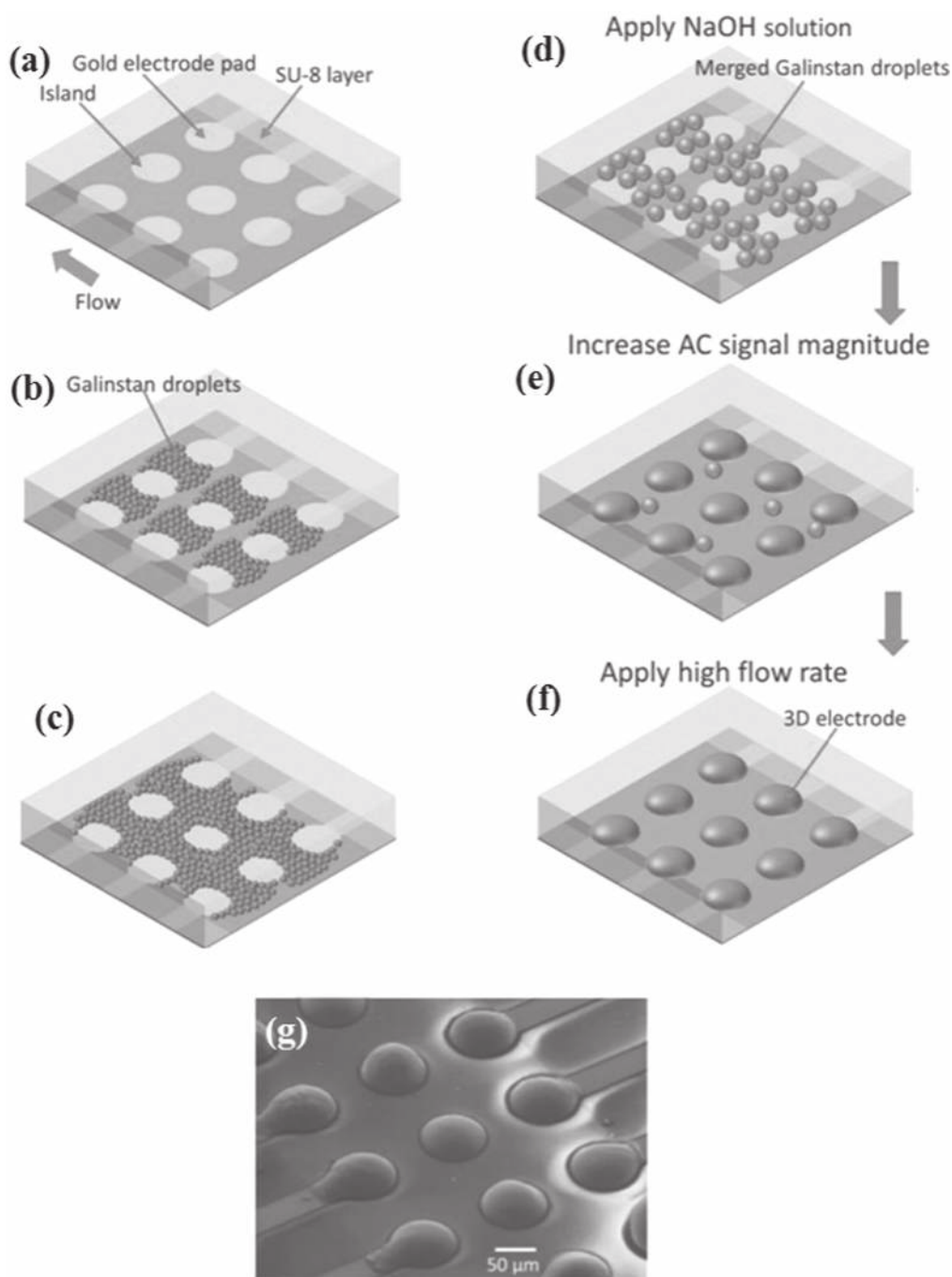
Figure 9. (a) The DEP platform with pairs of microelectrode pads and islands. Immobilization of liquid metal microdroplets by electrophoresis after (b) 10 s and (c) 20 s. (d) Application of NaOH solution and (e) increasing AC signal magnitude to merge microdroplets. (f) High flow rate is used to wash out the unmerged droplets and finally (f) the SEM image of liquid metal 3D microelectrodes using dielectropheresis (adapted from [94]. Copyright WILEY 2015 reprinted with permission).

channels. Then, one syringe is inserted at one end to inject the liquid metal and another syringe is inserted at other end to permit air to escape. Once the infiltration is done, the patterned liquid metal is frozen. Finally, if necessary, the solid structure can be embedded into elastomers. The steps involving needle injection casting are shown in the figure 11.

This freeze casting technique was developed to permit multiple independent electrodes and 3D liquid metal structures to be produced, removed (as solids), and then arranged in new positions prior to casting a new encapsulating PDMS layer. While necessitating much more manual operation to arrange electrodes in place, it was capable of producing multi-thickness electrodes with high dimensional accuracy at independent locations within a solid elastomer block. The major disadvantage of this technique is the requirement to do all solid metal handling at significantly reduced temperatures, necessitating a cold plate within a humidity controlled chamber to prevent condensation during
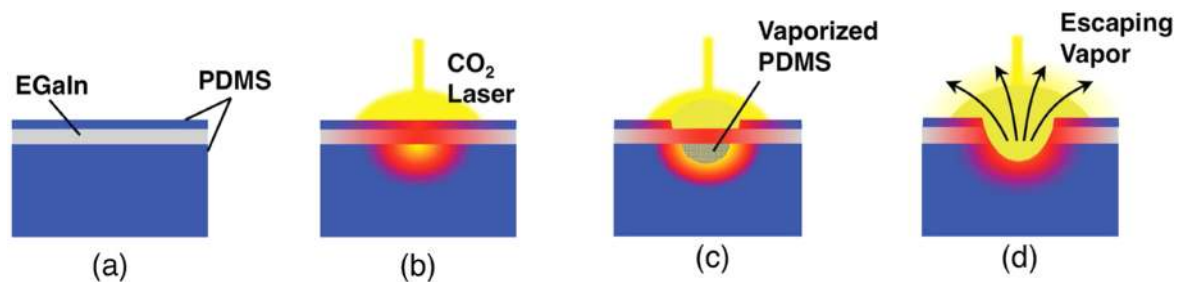
Figure 10. Direct patterning using laser. (a) Liquid metal encased between two PDMS layers, (b) application of CO_2 laser, (c) locally vaporized PDMS and (d) vapor escaping results patterned planar staructure (adapted from [95]. Copyright WILEY 2014 reprinted with permission).

the work. PDMS was cured at room temperature or higher as well, which meant that some complex features distorted as they were molten during the PDMS cure. A lower temperature curable PDMS, or alternative mechanisms such as UV curing could permit encapsulation while the alloy was still solid [97].

It is also possible to use an elastomer mold with enclosed 3D cavity instead of using glass plate to seal the top of the mold [96, 98–100]. Zhao *et al* used the same method with high pressure (~10 MPa) infiltration of liquid metal into hollow silica fiber and fabricated 150 nm diameter nanowires [85]. It is also possible to guide the liquid metal while filling with needle injection by using inherently aligned PDMS micro-pillars. *So and Dickey* fabricated devices by injecting liquid metal into 1000 μm wide channels between micro-pillars with only 50 μm spacing [99]. The oxide layer of liquid metal helps to flow along the electrode channel without leaking through the micro-pillars because of the very small gap between two neighboring micro-pillars compared to the width of the microfluidic channel. Needle injection method is a very fast, reliable and simple process. It can produce 3D structures with smoother sidewalls than most alternatives. One commonly faced problem is air trapping in complex structure during infiltration.

2.4.2. Vacuum assisted infiltration. Vacuum assisted casting is best when fabricating 3D deep features. This method eliminates the problem of air trapping with needle injection, particularly if sharp changes in thickness are desired. One variation of vacuum assisted casting was applied in conjunction with the freeze casting methods described earlier. As depicted in figure 12, in this technique an initially excess amount of liquid metal is poured onto the PDMS mold. Then using vacuum, any tapped air or air bubbles are removed but their passage through the metal will leave small holes in the liquid alloy. Once degassing is done, the liquid metal layer is reformed without holes by perturbation of the mold while maintaining the vacuum. Release from vacuum helps to fill the mold completely and excess materials can be removed by scraping the top surface. Finally, the liquid structure is frozen and the solid features removed for future embedding in a new PDMS casting.

An alternative vacuum assisted casting technique was described by Cumby *et al* who used a polyimide film with 0.4 μm vertical pores to fill a mold quickly with liquid metal [119]. Liquid metal is filled between the porous film and the mold. The required pressure for liquid metal to enter the submicron sized pores is very high, so only air is able to enter the pores and become evacuated rapidly throughout the whole area while applying suction. To increase horizontal degassing, a textile can also be introduced between the vacuum table and vertically porous film as shown in the figure 13.

This vacuum assisted infiltration has a higher filling rate compared to needle injection. But it also requires repeated process to ensure no air is trapped inside the complex structure with different channel height. The reported minimum feature size using vacuum assisted infiltration is 250 μm [119]. This technique is suitable for structures with deep features. Unlike needle injection, it does not need two terminals to allow air escaping and infiltration. This technique is very similar to the technique used in microsolidics by Siegel *et al* with low melting point metal (i.e. solder) [134]. Microsolidics basically uses techniques based on microfluidics, but ultimately develops solid metal structures. As an additional step, the inner surfaces of the microchannels were treated with plasma oxidation and silanization with 3-mercaptopropyltrimethoxysilane to decrease surface free energy enhancing the wettability by the molten metal.

3. Particularities and opportunities of liquid metal micro structures

While working with liquid metal, researchers have faced a number of challenges which limit its application. Some of these challenges have been overcome and reported by others. But still there are some opportunities for further research. In this section, all the difficulties and their reported solutions are described. It also includes the undone opportunities for future work.

3.1. Wetting property due to oxide layer

Gallium based liquid metals form a thin passivation oxide layer on all exposed surfaces when in contact with atmospheric oxygen. This oxide layer has high surface energy, which causes the liquid metal to wet almost any surface and complicates its liquid behavior as it has both fluid and solid
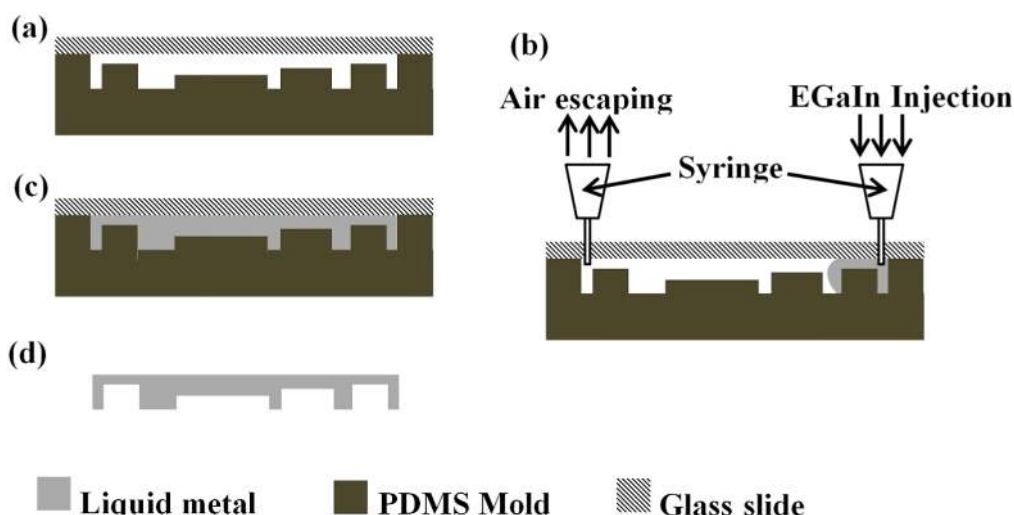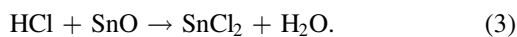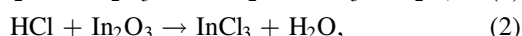
Figure 11. Needle injection of liquid metal. (a) The PDMS mold, (b) injection of liquid metal, (c) liquid metal filled channels and (d) solid structure of EGaIn (inspired by [97]).

like behaviors. From Pourbaix diagram [135], this amphoteric oxide can be removed by acidic environment (pH < 3) or basic environment (pH > 10) [136]. There are a number of reports where researchers successfully controlled the wettability of liquid metal and removed the oxide layer with techniques ranging from acid treatments, electrochemical reduction in electrolytes and even ultra-low oxygen environments [42].

3.1.1. Recovery of non-wetting characteristic by acid treatment. Though the oxide layer formed on liquid metal surface increases stability of the structures in mirochannels, it also causes viscoelasticity of the liquid metal resulting non-uniform shape and making the liquid metal behave as a non-Newtonian liquid. Firstly, Zrnic *et al* [78] and Dickey *et al* [55] successfully removed the oxide layer by treating with diluted hydrochloric acid (HCl) solution. The possible reactions of the acid with the metallic oxides in galinstan or EGaIn are as follows [137]:

$$HCl + Ga_2O + Ga_2O_3 \rightarrow GaCl_2 + GaCl_3 + H_2O, \quad (1)$$

$$HCl + In_2O_3 \rightarrow InCl_3 + H_2O, \quad (2)$$

$$HCl + SnO \rightarrow SnCl_2 + H_2O. \quad (3)$$

The primary reaction of importance is that of the gallium oxides to form gallium chlorides because gallium is the primary oxide formed on the liquid metals. Attractively, the chlorides that are formed do not have the same effects on liquid metal flow and wettability and permit the drop to behave more like a pure liquid. Later on, instead of using HCl solution, Kim *et al* [138] used HCl vapor to recover the non-wetting property of the liquid metal by keeping a pendant drop of HCl (37 wt%, ~5 μl) just 2 mm away from the liquid metal droplet for only 15 s. Before the HCl treatment, due to the oxide skin the drops of liquid metal had non-uniform shape with 127.6° contact angle on glass substrate, whereas after the treatment, the shape became uniform and contact angle increased to 139.5° on the same substrate. Kim *et al*

also performed a bouncing test, which illustrates the non-wetting property of liquid metal after HCl treatment. An HCl treated galinstan droplet of ~10 μl was dropped from 3.5 cm height onto a Teflon-coated glass. The droplet bounced back rather than sticking to the surface. The time-lapse images of the droplet can be found in [138]. Researchers removed the oxide by the acid treatment and were successful in their applications. These included demonstration of movement of liquid metal in microfluidic channel formed on HCl-impregnated paper [139] and a technique for selectively erasing and refilling unit cells of liquid metal based terahertz metamaterials [140].

Besides HCl, sulfuric acid (H_2SO_4) was also used to treat microfluidic channel inner walls to improve the non-wetting property of liquid metal [141]. Oxidized galinstan droplets were created, transported, separated and merged successfully in H_2SO_4 treated microfluidic channels, which demonstrates the possibility of reconfigurable applications.

3.1.2. Micro-texturing to control wettability. When a droplet of liquid metal is dropped on to any metallic surface, it may exhibit poor wetting with a very high contact angle or partial wetting with comparatively lower contact angle. Moreover, partial wetting has two cases, conventional partial wetting with no morphological change and partial wetting followed by reactive wetting with penetration in to grain boundaries. In the case of reactive wetting, contact angle changes to a very small equilibrium value, making the liquid metal completely spread over the substrate [142]. Kramer *et al* [143] have analyzed the wetting behaviors of liquid metal on bare and sputtered indium (In) and tin (Sn) foils. Analogous to controlling hydrophobicity of a surface by micro-texturing on it [144], the metallophobicity of the foil substrates can be controlled by the surface roughness resulting from the sputtering operation. Due to the lower indium percentage in galinstan (21.5%) compared to EGaIn (24.5%), galinstan was found to partially wet indium foil, whereas EGaIn highly wets. On the contrary, galinstan reactively wets tin foils
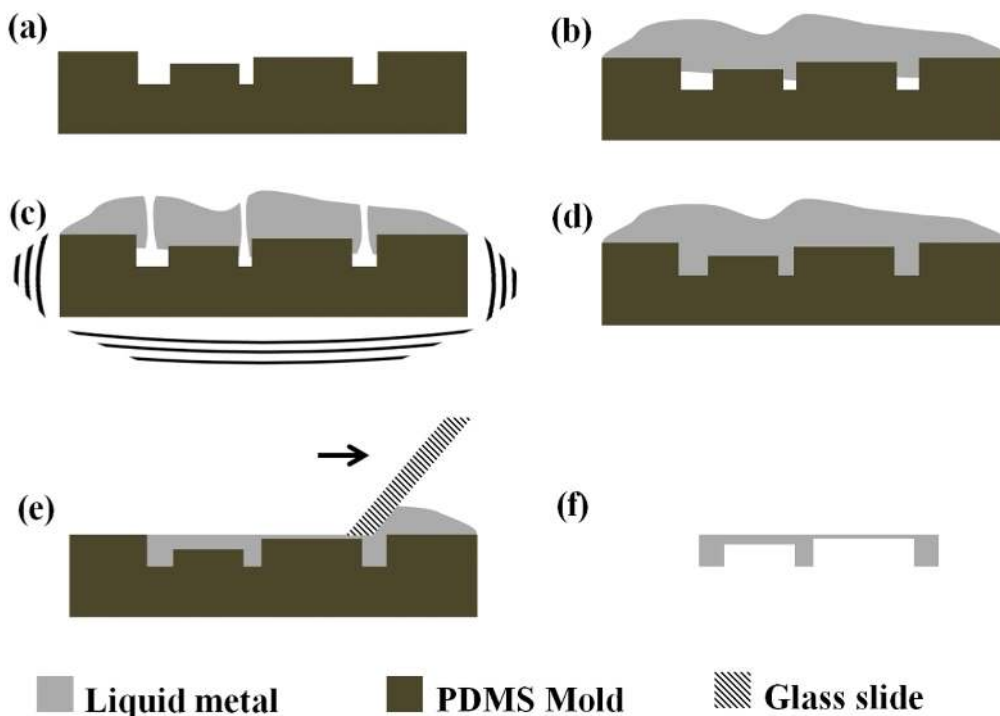
Figure 12. Vacuum assisted infiltration. (a) PDMS mold, (b) liquid metal is poured onto PDMS mold, (c) degassing in vacuum creates holes in liquid metal layer to help air escaping, and perturbation helps filling, (d) liquid metal is filled into channels, (e) excess amount of liquid metal is scraped and (f) after freezing the solid structure of EGaIn (inspired by [97]).
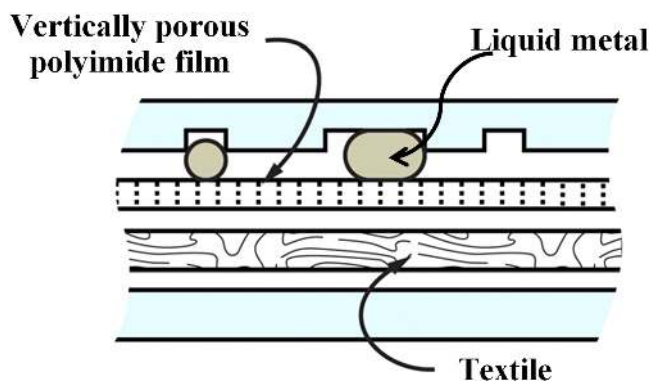

Figure 13. Approach for faster vacuum infiltration of liquid metal into PDMS mold (adapted from [119]. Copyright WILEY 2012 reprinted with permission).

Table 3. Wetting behavior of EGaIn/galinstan on to indium/tin substrates (*inspired by* [143]).

Liquid metal	Substrate material	Sputter material	Type of wetting
EGaIn	Silicon	Indium	No wetting
	Indium foil	Indium	Reactive wetting
	Tin foil	Indium	Partial wetting
Galinstan	Silicon	Tin	No wetting
	Indium foil	Tin	Partial wetting
	Tin foil	Tin	Reactive wetting

because of the presence of tin (10%) in galinstan. It has been confirmed using EDS, after reactive wetting the percentage of tin in that interaction zone increased to $19.68\% \pm 0.2\%$ [143]. The results are summarized in table 3.

Li *et al* demonstrated that a textured PDMS surface also enhances the non-wetting property of liquid metal [141]. First, the dual-scale micro-textures of normal A4 paper were transferred to the inner walls of PDMS micro-channels. Then, for further improvement, titanium oxide (TiO_2) nano-particles were coated on the micro-textured PDMS surfaces. It showed the highest advancing angle of $167°$ and lowest receding angle of $151°$, a low hysteresis of only $16°$. These results suggest the possibility of this surface modification for reconfigurable/tunable electronic applications.

3.1.3. Super-lyophobicity with multi-scale textured PDMS. There are some applications not requiring elimination of the oxide skin. Rather than removing the oxide layer, the non-wetting behavior of liquid metal can also be maintained even with the oxide present. Kim *et al* developed a super-lyophobic three dimensional PDMS channel to manipulate oxidized galinstan without wetting the surface [145]. Experiments to check the lyophobicity of modified PDMS surfaces in contact with already oxidized galinstan droplets were performed. These PDMS surfaces were textured with micropillars and/or microridges with or without a coating of fluoropolymers including Teflon and Cytop. It was found that the multi-scale textured PDMS micropillars with $75\,\mu m$ diameter and $100\,\mu m$ spacing coated with fluorocarbon polymer experience super-lyophobicity. It has static contact angle of $156.9°$, which is beyond the super-lyophobic regime of $150°$.

In addition, it is believed that another reason of this super-lyophobicity is the low solid-fraction (f_s) due to the additional surface roughness of the multi-scale textured micropillars.

3.1.4. CNT based super-lyophobic surface.

Kim *et al* reported that a vertically aligned carbon nanotube (CNT) forest can contribute to maintain lyophobicity of the PDMS surface in contact with galinstan [146]. Hierarchical micro/nano scale combined structure of CNT is proved to have super-repellent property in contact with oil or water [147–150]. First, the vertically aligned CNT was grown using chemical vapor deposition (780 °C, 5 min) on an iron coating (6 nm thick) deposited by e-beam evaporation on SiO_2/Si substrate. Then, a nano-imprinter was used to transfer the CNT forest from the Si substrate to PDMS sheet. Finally the static contact angle, dynamic contact angle, bouncing test and rolling test of galinstan droplet were measured and performed with (i) CNT on Si substrate, (ii) CNT on PDMS sheet with 0%, 50% and 100% stretching and (iii) CNT on PDMS with 0.1 and 0.4 mm^{-1} curvature. Rolling tests of 7.8 and 1.6 μl droplets on curved PDMS sheets with CNT forest were performed by Kim *et al*, which prove the non-wetting behavior of galinstan as no residue was seen on the surfaces after rolling tests.

3.2. Critical dimension and line edge roughness

In microfabrication, the resolution and precision of patterning structures are characterized on the basis of two significant criteria, critical dimension [151] and line edge roughness [152]. Critical dimension is the size of the smallest possible feature fabricated and line edge roughness measures the edge deviations of a critical dimension. A number of techniques discussed in this review result in higher edge roughness. Except for needle injection and imprinting using molds, no other technique has been reported to fabricate features smaller than the micrometer range. Most of the techniques can develop patterns on the order of 100 μm in minimum dimension. Casting by needle injection and vacuum assisted filling produce relatively smooth walls and lines (which are primarily determined by the original molding process used to make the channels) when compared to all direct printing or patterning methods described to date. Pure liquid gallium was found inside CNT [153, 154], which means it may be possible to produce finer features of liquid metal. Further research is required to enhance the resolution of the liquid metal structures by fabricating even smaller features in submicron scale.

3.3. 3D freestanding microstructures

Though the three-dimensional freestanding microstructures have been produced by Ladd *et al* [72], they have not yet been utilized in any application. These structures also have issues with stability, repeatability etc. To overcome these issues, the additive technique, 3D printing may be useful to fabricate liquid metal structures embedded in 3D printable elastomers or plastics. *Wang* and *Liu* utilized liquid phase 3D printing using the $Bi_{35}In_{48.6}Sn_{15.9}Zn_{0.4}$ alloy to quickly fabricate conductive metal objects with the help of cooling fluid to prevent oxidation [155, 156]. The liquid phase 3D printing technique by *Wang* and *Liu* might be adopted to print liquid metal alloy. However, it remains to be proven how well the 3D patterns can be utilized in real-life applications.

3.4. Reconfigurability

Reconfigurable electronics refer to adaptive, multifunctional future devices for information and communications technology. Conventional reconfigurable devices use mechanical switches, transistors, diodes, or varactors to change the radiofrequency (RF) properties (e.g. resonant wavelength) by dynamically altering the static layout of electrical interconnects [157]. However, these conventional approaches have a limited variability and range of states. More versatile devices with the ability to dynamically reconfigure, tune, erase or write electrical circuits are possible if incorporating liquid metal components. Recently, the use of liquid metal in reconfigurable microstrip RF filters [158, 159], wideband RF switches [160], FSS [161], antennas [98, 162–166] and plasmonic devices [167] have been reported. In these applications, though the control of current paths is significantly enhanced by pneumatically actuating liquid metal using pumps or contact pressure, the use of an external control system increases overall complexity, reduces switching speed and is unable to reconfigure actual wires. These limitations can be overcome by enabling continuous electrowetting (CEW) [168] or Laplace pressure shaping [119] to actuate liquid metal in a capillary.

Researchers are still working on the shape reconfigurability. Due to the oxide skin, some residual amount of liquid metal remains in the channel even after evacuating that. Acid vapor treated surfaces [67, 164, 169], lyophobic surfaces [145, 146, 170], micro-textured surfaces [142, 143] discussed in section 3.1 can be useful to control the wettability of liquid metal in reconfigurable devices and eliminate this residual material. However, the use of harsh chemicals (e.g. acid vapor) may not be desirable in many applications. In addition, surface modification requires some additional steps and increases overall process complexity. Other successful research on enhancing reconfigurability of liquid metals is discussed below.

3.4.1. Use of carrier fluid.

A simple method to prevent wetting of microchannels by liquid metal is to use an aqueous solution of 20 wt% poly (ethylene glycol) and 5 wt% sodium dodecyl sulfate [171]. The solution acts as carrier fluid of liquid metal by assisting in forming microdroplets of liquid metal and maintains their spherical or non-spherical shape within microfluidic channels without adhering to each other and channel wall. Though this water based technique is useful in reconfigurable applications, water is not ideal for RF applications due to its high loss at high RF frequencies.

In addition to the use of carrier fluid, surface modification of the channel walls would also enhance the non-wetting property of the liquid metal. For instance, Koo *et al* investigated the use of carrier fluid in microchannels coated

with other materials to minimize EGaIn fragmentation and EGaIn residues on PDMS-based microfluidic channels during repeated actuation of an EGaIn plug for tunable RF applications [172]. It was found that a PDMS microchannel coated with 2% of nonionic surfactant TWEEN 20 (Sigma, Saint Louis, MO) or 5% of hydrophobic PTFE resulted in no residue of liquid metal even with repeated flow when using high viscosity oil (Hydrocal 2400) as a carrier fluid. The stable result confirms the fulfilment of the requirement for repeated reconfiguration of RF devices.

In another method, Khan *et al* used water as an interfacial slip layer in microchannel, which allows the liquid metal successfully to flow across the channel surfaces without sticking to it [173]. The microchannel was first prefilled with water, and then the liquid metal plug was injected. The water slip layer acts as a lubricant and allows CEW of the plug [174]. Unfortunately, the water evaporates relatively quickly, and after 10–12 min, there was insufficient water lubrication to prevent direct contact of the liquid metal with the channel sidewalls and the slipping behavior was lost.

3.4.2. Recapillarity.

Oxidation increases the surface tension of gallium based liquid metal alloys. For instance, the EGaIn droplet with oxide skin has an effective surface tension of around $624 \, mN \, m^{-1}$ [78] but will highly wet surfaces when the oxide is breached, whereas the oxide-free droplet has only $435 \, mN \, m^{-1}$ surface tension [42, 77] but can be non-wetting if the oxide formation is suppressed. Therefore, the oxide skin acts as an intrinsic 'surfactant'. The formation of oxide skin has been regulated by electrochemically depositing or removing with help of very small voltage (<1 V) [57]. Hence, the interfacial surface tension of liquid metal droplet was controlled using potential—that is, electrocapillarity. Tang *et al* successfully steered liquid metal flow in microchannel using low voltages [175]. Khan *et al* also successfully controlled the flow direction of liquid metal in a microchannel by application of a voltage in the presence of 1 M NaOH [57]. It was found that the oxide skin can be removed by applying a modest reductive voltage (e.g. −1 V) to induce capillary behavior. The introduction of capillary behavior of liquid metal by applying reductive voltage is termed as 'recapillarity' [57, 176]. Recapillarity enables liquid metal to flow in microchannel without leaving any residue (figure 14), which is the requirement of reconfigurable electronics applications. The biggest disadvantage of the electrochemistry is the need of a continuous power supply to maintain oxide-free metal.

3.5. Damaging nature of liquid metal

The damaging nature of liquid gallium on metals and alloys was observed by Deng and Liu [177], but this issue can be resolved using contactless geometry [178]. Not only the liquid gallium, but galinstan and EGaIn alloys will also have this ability to damage metals, which can be avoided using a multilayer graphene diffusion barrier [179]. However the issue with corrosive nature of these liquid metals is something
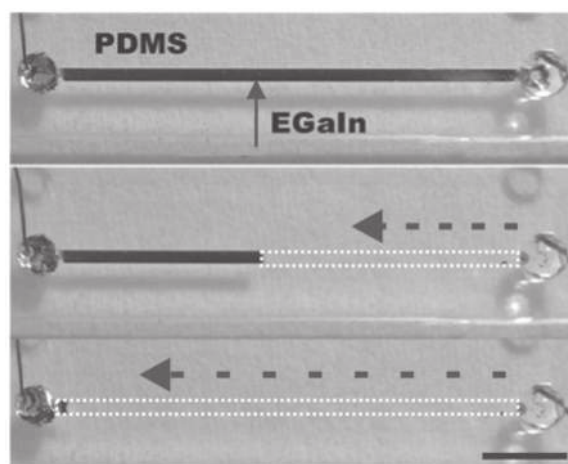

Figure 14. Recapillarity in action. The liquid metal is withdrawn by applying small voltage without leaving any residue in microchannel (adapted from [176]. Copyright WILEY 2014 reprinted with permission).

that has not been fully addressed in the literature and may have implications for long term use of these materials. It is believed that, this is the amalgamation effect, for which the alloying process starts when liquid metal is in contact with other metals. It results in a new alloy with different composition accompanied by the damage or destruction of the original solid metal.

To demonstrate the damaging nature of galinstan, tested several small pieces of different materials as summarized in table 4 and shown in figure 15. We kept the samples in contact with galinstan for different lengths of time and at different temperatures. It was found that galinstan starts damaging the aluminium samples within 5 min and it completely destroys the aluminium samples in around 30 min even in room temperature. Compared to aluminium, brass showed less vulnerability with galinstan. At room temperature, no noticeable damage was seen in brass samples up to 24 h. But it starts damaging the brass samples in about 5 min when heated at ~100 °C, whereas at 230 °C, brass sample was completely destroyed by galinstan within 3 h. Copper samples also did not show any noticeable damage while keeping in contact with galinstan at room temperature up to 24 h. But at higher temperature copper samples were damaged in galinstan over time, it took approximately one hour to dissolve completely at 230 °C. Among them, stainless steel showed superior resistance to galinstan. The washers made of stainless steel were not damaged even after 5 h of heating at 230 °C. Physically, it only changes the appearance to a reddish color. SEM images of non-exposed washer and exposed washer (230 °C for 5 h) also confirm no significant change in surface topology. Therefore, for low temperature applications, brass electrodes might serve the purpose of external wiring but for higher temperature applications, stainless steel would be better choice. Aluminium is not recommended for this wiring purpose regardless of the working temperature.

Table 4. Summary of the results of experiments to check the damaging nature of liquid metal with common solid metals at room temperature (RT) and elevated temperatures.

Materials	Samples	Damaged in:	Destroyed in:
Aluminium	Tubes (OD: 1.6 mm, ID: 0.9 mm and length: 4 mm)	5 min at RT;	30 min at RT;
Brass (C36000)	Tubes (OD: 1.6 mm, ID: 0.9 mm and length: 4 mm)	24 h at RT; 5 min at 100 °C;	3 h at 230 °C;
Copper	Rectangular sheet (3 mm × 3 mm × 0.12 mm)	24 h at RT;	1 h at 230 °C;
Stainless steel (316)	Washer (OD: 7 mm, ID: 3.2 mm, and thickness: 0.65 mm)	5 h at 230 °C	—

Figure 15. (a) Non-exposed aluminium sample, exposed aluminium sample for (b) 15 min at room temperature, (c) 5 min at 100 °C, (d) completely desolved aluminium at room temperature for 30 min (e) Non-exposed brass sample, (f) exposed brass sample for 5 min at 100 °C, (g) exposed brass sample for 2 h at 230 °C (h) completely desolved brass for 3 h at 230 °C (i) Non-exposed Cu sample, (j) exposed Cu sample for 15 min at 100 °C, (k) exposed Cu sample for 30 min at 230 °C, (l) completely corroded Cu sample after 1 h at 230 °C and (m) non-exposed 316-stainless steel washer (right) & exposed washer (left) for 5 h at 230 °C.

To overcome the challenge with direct-contact damage by liquid metal, co-axial extrusion of liquid metal wires already encapsulated in thermoplastic shell might be a part of the future work. Still it should be considered that higher temperature exposures for these liquid metals may lead to damage to the extrusion die.

4. Discussion and conclusion

Liquid metals can be processed with a variety of techniques to produce 2D or 3D microstructures embedded in elastomeric materials to perform as a highly stretchable, flexible, light weight, self-healing devices with comparable conductivity with metals like Cu, Au etc. This report highlights the recent research on liquid metals and their fabrication processes to aid those interested in manufacturing new stretchable, electronically functional smart materials. All the available fabrication techniques are grouped into four major categories such as masked deposition, imprinting, direct patterning and casting. In each major category there are a number of techniques involving different methods to develop liquid metal structures. In this report, a total of 12 different fabrication techniques with their unique advantages and disadvantages have been discussed. The minimum feature size reported using the corresponding techniques have also been summarized in table 2. Needle injection and direct 3D patterning are the currently available processes for three-dimensional structures. On the other hand, imprinting and masked deposition processes are dedicated for planar structures. Imprinting using a mold and stamp are the simplest processes to fabricate 2D structures but imprinting using a stamp is limited for relatively large features (~750 μm). The techniques reported up to now have relatively poor resolution compared to the conventional microfabrication techniques for polymers. The biggest challenge is, coercing the liquid metal into micro/nano sized feature because of the oxide skin and large surface tension. But pure liquid gallium inside CNT has been studied, which suggests a new horizon of possibility to create finer features of liquid metal.

After fabricating the functional structure, suitable wiring plays an important role in utilizing the designs in their applications. Most applications require connecting the liquid metal with other conductive components for electrical contacts. Gallium alloys with other materials, which may limit its use with a variety of possible electrode materials. For instance, if an aluminium thin film is used in direct contact with gallium based alloys, aluminium readily is corroded even at room temperature. This phenomenon may be prevented using a multilayer graphene diffusion barrier or selection of chemically resistant metallic electrodes but needs to be considered for the expected lifetime and temperature range of the expected liquid metal application.

References

[1] Khang D Y, Jiang H, Huang Y and Rogers J A 2006 A stretchable form of single-crystal silicon for high-performance electronics on rubber substrates *Science* **311** 208–12

[2] Sun Y and Rogers J A 2007 Inorganic semiconductors for flexible electronics *Adv. Mater.* **19** 1897–916

[3] Unsworth J, Conn C, Jin Z, Kaynak A, Ediriweera R, Innis P and Booth N 1994 Conducting polymers: properties and applications *J. Intell. Mater. Syst. Struct.* **5** 595–604

[4] Yang S and Ruckenstein E 1993 Preparation and mechanical properties of electrically conductive polypyrrole-poly (ethylene-co-vinyl acetate) composites *Synth. Met.* **60** 249–54

[5] Jung H C, Moon J H, Baek D H, Lee J H, Choi Y Y, Hong J S and Lee S H 2012 CNT/PDMS composite flexible dry electrodes for long-term ECG monitoring *IEEE Trans. Biomed. Eng.* **59** 1472–9

[6] Liu C X and Choi J W 2010 Strain-dependent resistance of PDMS and carbon nanotubes composite microstructures *IEEE Trans. Nanotechnol.* **9** 590–5

[7] Khosla A and Gray B L 2009 Preparation, characterization and micromolding of multi-walled carbon nanotube polydimethylsiloxane conducting nanocomposite polymer *Mater. Lett.* **63** 1203–6

[8] Chen M, Tao T, Zhang L, Gao W and Li C 2013 Highly conductive and stretchable polymer composites based on graphene/MWCNT network *Chem.Commun.* **49** 1612–4

[9] Chen Z, Xu C, Ma C, Ren W and Cheng H M 2013 Lightweight and flexible graphene foam composites for high-performance electromagnetic interference shielding *Adv. Mater.* **25** 1296–300

[10] Hu W, Niu X, Li L, Yun S, Yu Z and Pei Q 2012 Intrinsically stretchable transparent electrodes based on silver-nanowire-crosslinked-polyacrylate composites *Nanotechnology* **23** 344002

[11] Cong H and Pan T 2008 Photopatternable conductive PDMS materials for microfabrication *Adv. Funct. Mater.* **18** 1912–21

[12] Niu X, Peng S, Liu L, Wen W and Sheng P 2007 Characterizing and patterning of PDMS-based conducting composites *Adv. Mater.* **19** 2682–6

[13] Khondoker M A H, Yang S Y, Mun S C and Kim J 2012 Flexible and conductive ITO electrode made on cellulose film by spin-coating *Synth. Met.* **162** 1972–6

[14] Seyedin M Z, Razal J M R, Innis P C and Wallace G G 2014 Strain-responsive polyurethane/PEDOT:PSS elastomeric composite fibers with high electrical conductivity *Adv. Funct. Mater.* **24** 2957–66

[15] Yin Z P, Huang Y A, Bu N B, Wang X M and Xiong Y L 2010 Inkjet printing for flexible electronics: materials, processes and equipments *Chin. Sci. Bull.* **55** 3383–407

[16] Ko S H, Pan H, Grigoropoulos C P, Luscombe C K, Frechet J M and Poulikakos D 2007 All-inkjet-printed flexible electronics fabrication on a polymer substrate by low-temperature high-resolution selective laser sintering of metal nanoparticles *Nanotechnology* **18** 345202

[17] Khondoker M A H, Mun S C and Kim J 2013 Particle based conductive silver ink customized for ink jet printing on cellulose electro-active paper *Proc. SPIE* **8691** 86910Q

[18] Stoyanov H, Kollosche M, Risse S, Wache R and Kofod G 2013 Soft conductive elastomer materials for stretchable electronics and voltage controlled artificial muscles *Adv. Mater.* **25** 578–83

[19] Hosoda K, Tada Y and Asada M 2006 Anthropomorphic robotic soft fingertip with randomly distributed receptors *Robot. Auton. Syst.* **54** 104–9

[20] Cagatay E, Kohler P, Lugli P and Abdellah A 2015 Flexible capacitive tactile sensors based on carbon nanotube thin films *IEEE Sensors J.* **15** 3225–33

[21] Lee H K, Chang S I and Yoon E 2006 A flexible polymer tactile sensor: fabrication and modular expandability for large area deployment *J. Microelectromech. Syst.* **15** 1681–6

[22] Kuo C M, Lin C H and Huang Y C 2005 Plastic deformation mechanism of pure copper at low homologous temperatures *Mater. Sci. Eng. A* **396** 360–8

[23] Rogers J A, Someya T and Huang Y 2010 Materials and mechanics for stretchable electronics *Science* **327** 1603–7

[24] Rojas J P, Hussain A M, Arevalo A, Foulds I G, Torres Sevilla G A, Nassar J M and Hussain M M 2015 Transformational electronics are now reconfiguring *Proc. SPIE* **9467** 946709

[25] Befahy S, Yunus S, Pardoen T, Bertrand P and Troosters M 2007 Stretchable helical gold conductor on silicone rubber microwire *Appl. Phys. Lett.* **91** 141911

[26] Brosteaux D, Axisa F, Gonzalez M and Vanfleteren J 2007 Design and fabrication of elastic interconnections for stretchable electronic circuits *IEEE Electron Device Lett.* **28** 552–4

[27] Gonzalez M, Axisa F, Bulcke M V, Brosteaux D, Vandevelde B and Vanfleteren J 2008 Design of metal interconnects for stretchable electronic circuits *Microelectron. Reliab.* **48** 825–32

[28] Huyghe B, Rogier H, Vanfleteren J and Axisa F 2008 Design and manufacturing of stretchable high-frequency interconnects *IEEE Trans. Adv. Packag.* **31** 802–8

[29] Gray D S, Tien J and Chen C S 2004 High-conductivity elastomeric electronics *Adv. Mater.* **16** 393–7

[30] Miller M S, Davidson G J E, Sahli B J, Mailloux C M and Carmichael T B 2008 Fabrication of elastomeric wires by selective electroless metallization of poly(dimethylsiloxane) *Adv. Mater.* **20** 59–64

[31] Morent R *et al* 2007 Adhesion enhancement by a dielectric barrier discharge of PDMS used for flexible and stretchable electronics *J. Phys. D: Appl. Phys.* **40** 7392–401

[32] Rosset S, Niklaus M, Dubois P and Shea H R 2009 Metal ion implantation for the fabrication of stretchable electrodes on elastomers *Adv. Funct. Mater.* **19** 470–8

[33] Kim J *et al* 2015 Epidermal electronics with advanced capabilities in near-field communication *Small* **11** 906–12

[34] Huang X, Liu Y, Chen K, Shin W, Lu C, Kong G, Patnaik D, Lee S, Cortes J F and Rogers J A 2014 Stretchable, wireless sensors and functional substrates for epidermal characterization of sweat *Small* **10** 3083–90

[35] Huang X *et al* 2014 Materials and designs for wireless epidermal sensors of hydration and strain *Adv. Funct. Mater.* **24** 3846–54

[36] Gao L *et al* 2014 Epidermal photonic devices for quantitative imaging of temperature and thermal transport characteristics of the skin *Nat. Commun.* **5** 4938

[37] Kim D *et al* 2011 Epidermal electronics *Science* **333** 838–43

[38] Rahimi R, Ochoa M, Yu W and Ziaie B 2014 A sewing-enabled stitch-and-transfer method for robust, ultra-stretchable, conductive interconnects *J. Micromech. Microeng.* **24** 095018

[39] Wang X, Hu H, Shen Y, Zhou X and Zheng Z 2011 Stretchable conductors with ultrahigh tensile strain and stable metallic conductance enabled by prestrained polyelectrolyte nanoplatforms *Adv. Mater.* **23** 3090–4

[40] Whitney R J 1953 The measurement of volume changes in human limbs *J. Physiol.* **121** 1–27

[41] Beni G, Hackwood S and Jackel J L 1982 Continuous electrowetting effect *Appl. Phys. Lett.* **40** 912–4

[42] Liu T, Sen P and Kim C J 2012 Characterization of nontoxic liquid-metal alloy galinstan for applications in microdevices *J. Microelectromech. Syst.* **21** 443–50

[43] Winter T G 2003 The evaporation of a drop of mercury *Am. J. Phys.* **71** 783–6

[44] Furr A K 2000 *CRC Handbook of Laboratory Safety* (Boca Raton, FL: CRC Press) p 808

[45] Cheng S and Wu Z 2012 Microfluidic electronics *Lab Chip* **12** 2782–91

[46] Lide D R 2007 *CRC Handbook of Chemistry and Physics* (United Kingdom: CRC Press)

[47] Chandler J E, Messer H H and Ellender G 1994 Cytotoxicity of gallium and indium ions compared with mercuric ion *J. Dent. Res.* **73** 1554–9

[48] Joshipura I D, Ayers H R, Majidi C and Dickey M D 2015 Methods to pattern liquid metals *J. Mater. Chem.* C **3** 3834–41

[49] Mott N F 1934 The resistance of liquid metals *Proc. R. Soc.* A **146** 465–72

[50] Scharmann F, Cherkashinin G, Breternitz V, Knedlik C, Hartung G, Weber T and Schaefer J A 2004 Viscosity effect on GaInSn studied by XPS *Surf. Interface Anal.* **36** 981–5

[51] Sangeeth C S S, Wan A and Nijhuis C A 2014 Equivalent circuits of a self-assembled monolayer-based tunnel junction determined by impedance spectroscopy *J. Am. Chem. Soc.* **136** 11134–44

[52] Regan M J, Tostmann H, Pershan P S, Magnussen O M, DiMasi E, Ocko B M and Deutsch M 1997 X-ray study of the oxidation of liquid-gallium surfaces *Phys. Rev.* B **55** 10786–90

[53] Plech A, Klemradt U, Metzger H and Peisl J 1998 *In situ* x-ray reflectivity study of the oxidation kinetics of liquid gallium and the liquid alloy $Ga_{0.93}Hg_{0.07}$ *J. Phys. Condens. Matter* **10** 971

[54] Cademartiri L *et al* 2012 Electrical resistance of Ag^{TS}-S $(CH_2)_{n-1}CH_3//Ga_2O_3$/EGaIn tunneling junctions *J. Phys. Chem.* C **116** 10848–60

[55] Dickey M D, Chiechi R C, Larsen R J, Weiss E A, Weitz D A and Whitesides G M 2008 Eutectic gallium–indium (EGaIn): a liquid metal alloy for the formation of stable structures in microchannels at room temperature *Adv. Funct. Mater.* **18** 1097–104

[56] Chabala J M 1992 Oxide-growth kinetics and fractal-like patterning across liquid gallium surfaces *Phys. Rev.* B **46** 11346–57

[57] Khan M R, Eaker C B, Bowden E F and Dickey M D 2014 Giant and switchable surface activity of liquid metal via surface oxidation *Proc. Natl Acad. Sci. USA* **111** 14047–51

[58] Chiechi R C, Weiss E A, Dickey M D and Whitesides G M 2008 Eutectic gallium–indium (EGaIn): a moldable liquid metal for electrical characterization of self-assembled monolayers *Angew. Chem. Int. Ed.* **47** 142–4

[59] Doudrick K, Liu S, Mutunga E M, Klein K L, Damle V, Varanasi K K and Rykaczewski K 2014 Different shades of oxide: from nanoscale wetting mechanisms to contact printing of gallium-based liquid metals *Langmuir* **30** 6867–77

[60] Irshad W and Peroulis D 2009 A silicon-based galinstan magnetohydrodynamic pump *PowerMEMS: Proc. 9th Int. Workshop on Micro and Nanotechnology for Power Generation and Energy Conversion Applications (Washington DC, USA)* pp 127–9

[61] Eddings M A and Gale B K 2006 A PDMS-based gas permeation pump for on-chip fluid handling in microfluidic devices *J Micromech. Microeng.* **16** 2396

[62] Lazar I M and Karger B L 2002 Multiple open-channel electroosmotic pumping system for microfluidic sample handling *Anal. Chem.* **74** 6259–68

[63] Grover W H, Skelley A M, Liu C N, Lagally E T and Mathies R A 2003 Monolithic membrane valves and diaphragm pumps for practical large-scale integration into glass microfluidic devices *Sensors Actuators* B **89** 315–23

[64] Hansson T and Sjolander S 1997 Valve, especially for fluid handling bodies with microflowchannels *US Patent* US5593130 A

[65] Tang S, Khoshmanesh K, Sivan V, Petersen P, O'Mullane A P, Abbott D, Mitchell A and Kalantar-zadeh K 2014 Liquid metal enabled pump *Proc. Natl Acad. Sci. USA* **111** 3304–9

[66] Gao M and Gui L 2014 A handy liquid metal based electroosmotic flow pump *Lab Chip* **14** 1866–72

[67] Kim D, Yoo J H, Choi W, Yoo K and Lee J 2014 Real-time dynamically reconfigurable liquid metal based photolithography *27th Int. Conf. on Micro Electro Mechanical Systems (San Francisco, CA, USA)* IEEE p 540

[68] Kim D and Rogers J A 2008 Stretchable electronics: materials strategies and devices *Adv. Mater.* **20** 4887–92

[69] Li M, Yu B and Behdad N 2010 Liquid-tunable frequency selective surfaces *IEEE Microw. Compon. Lett.* **20** 423–5

[70] Gmati I E, Calmon P F, Ali B, Pons P, Fulcrand R, Pinon S, Boussetta H, Kallala M A and Besbes K 2011 Fabrication and evaluation of an on-chip liquid micro-variable inductor *J. Micromech. Microeng.* **21** 025018

[71] Knoblauch M, Hibberd J M, Gray J C and van Bel A J E 1999 A galinstan expansion femtosyringe for microinjection of eukaryotic organelles and prokaryotes *Nat. Biotechnol.* **17** 906–9

[72] Ladd C, So J H, Muth J and Dickey M D 2013 3D printing of free standing liquid metal microstructures *Adv. Mater.* **25** 5081–5

[73] Vetrovec J, Litt A S, Copeland D A, Junghans J and Durkee R 2013 Liquid metal heat sink for high-power laser diodes *Proc. SPIE* **8605** 86050E

[74] Hodes M, Rui Z, Lam L S, Wilcoxon R and Lower N 2014 On the potential of galinstan-based minichannel and minigap cooling *IEEE Trans. Compon. Packag. Manuf. Technol.* **4** 46–56

[75] Ma K Q and Liu J 2007 Nano liquid-metal fluid as ultimate coolant *Phys. Lett.* A **361** 252–6

[76] Kim H, Maleki T, Wei P and Ziaie B 2009 A biaxial stretchable interconnect with liquid-alloy-covered joints on elastomeric substrate *J. Microelectromech. Syst.* **18** 138–46

[77] Larsen R J, Dickey M D, Whitesides G M and Weitz D A 2009 Viscoelastic properties of oxide-coated liquid metals *J. Rheol.* **53** 1305–26

[78] Zrnic D and Swatik D S 1969 On the resistivity and surface tension of the eutectic alloy of gallium and indium *J. Less-Common Met.* **18** 67–8

[79] Surmann P and Zeyat H 2005 Voltammetric analysis using a self-renewable non-mercury electrode *Anal. Bioanal. Chem.* **383** 1009–13

[80] Aqra F and Ayyad A 2011 Theoretical calculations of the surface tension of liquid transition metals *Metall. Mater. Trans.* B **42** 5–8

[81] Takahashi K, Yoshikawa A and Sandhu A 2007 *Wide Bandgap Semiconductors: Fundamental Properties and Modern Photonic and Electronic Devices* (Berlin: Springer)

[82] Miller P H 1941 The electrical conductivity of zinc oxide *Phys. Rev.* **60** 890–5

[83] Osagawara M, Funahashi K, Demura T, Hagiwara T and Iwata K 1986 Enhancement of electrical conductivity of polypyrrole by stretching *Synth. Met.* **14** 61–9

[84] Jeong S H, Hagman A, Hjort K, Jobs M, Sundqvist J and Wu Z 2012 Liquid alloy printing of microfluidic stretchable electronics *Lab Chip* **12** 4657–64

[85] Zhao W *et al* 2015 Single-fluxon controlled resistance switching in centimeter-long superconducting gallium–indium eutectic nanowires *Nano Lett.* **15** 153–8

[86] Roberts P, Damian D D, Shan W, Lu T and Majidi C 2013 Soft-matter capacitive sensor for measuring shear and pressure deformation *IEEE Int. Conf. on Robotics and Automation (Karlsruhe, Germany)* pp 3529–34

[87] Tabatabai A, Fassler A, Usiak C and Majidi C 2013 Liquid-phase gallium–indium alloy electronics with microcontact printing *Langmuir* **29** 6194–200

[88] Kramer R K, Majidi C and Wood R J 2013 Masked deposition of gallium–indium alloys for liquid-embedded elastomer conductors *Adv. Funct. Mater.* **23** 5292–6

[89] Gozen B A, Tabatabai A, Ozdoganlar O B and Majidi C 2014 High-density soft-matter electronics with micron-scale line width *Adv. Mater.* **26** 5211–6

[90] Truong T D 2000 *Selective Deposition of Micro Scale Liquid Gallium Alloy Droplets* (Los Angeles, CA: University of California)

[91] Kim D, Yoo J H, Lee Y, Choi W, Yoo K and Lee J-B 2014 Gallium-based liquid metal inkjet printing *IEEE 27th Int. Conf. on Micro Electro Mechanical Systems (San Francisco, CA)* pp 967–70

[92] Boley J W, White E L, Chiu G T and Kramer R K 2014 Direct writing of gallium–indium alloy for stretchable electronics *Adv. Funct. Mater.* **24** 3501–7

[93] Zheng Y, He Z, Yang J and Liu J 2014 Personal electronics printing via tapping mode composite liquid metal ink delivery and adhesion mechanism *Sci. Rep.* **4** 4588

[94] Tang S, Zhu J, Sivan V, Gol B, Soffe R, Zhang W, Mitchell A and Khoshmanesh K 2015 Creation of liquid metal 3D microstructures using dielectrophoresis *Adv. Funct. Mater.* **25** 4445–52

[95] Lu T, Finkenauer L, Wissman J and Majidi C 2014 Rapid prototyping for soft-matter electronics *Adv. Funct. Mater.* **24** 3351–6

[96] Kim H, Son C and Ziaie B 2008 A multiaxial stretchable interconnect using liquid-alloy-filled elastomeric microchannels *Appl. Phys. Lett.* **92** 011904

[97] Fassler A and Majidi C 2013 3D structures of liquid-phase GaIn alloy embedded in PDMS with freeze casting *Lab Chip* **13** 4442–50

[98] So J, Thelen J, Qusba A, Hayes G J, Lazzi G and Dickey M D 2009 Reversibly deformable and mechanically tunable fluidic antennas *Adv. Funct. Mater.* **19** 3632–7

[99] So J and Dickey M D 2011 Inherently aligned microfluidic electrodes composed of liquid metal *Lab Chip* **11** 905–11

[100] Cheng S, Wu Z, Hallbjorner P, Hjort K and Rydberg A 2009 Foldable and stretchable liquid metal planar inverted cone antenna *IEEE Trans. Antennas Propag.* **57** 3765–71

[101] Fassler A and Majidi C 2013 Soft-matter capacitors and inductors for hyperelastic strain sensing and stretchable electronics *Smart Mater. Struct.* **22** 055023

[102] Liu S, Sun X, Hildreth O J and Rykaczewski K 2015 Design and characterization of a single channel two-liquid capacitor and its application to hyperelastic strain sensing *Lab Chip* **15** 1376–84

[103] Pekas N, Zhang Q and Juncker D 2012 Electrostatic actuator with liquid metal–elastomer compliant electrodes used for on-chip microvalving *J. Micromech. Microeng.* **22** 097001

[104] Kubo M, Li X, Kim C, Hashimoto M, Wiley B J, Ham D and Whitesides G M 2010 Stretchable microfluidic radiofrequency antennas *Adv. Mater.* **22** 2749–52

[105] Cheng S and Wu Z 2010 Microfluidic stretchable RF electronics *Lab Chip* **10** 3227–34

[106] So J, Koo H, Dickey M D and Velev O D 2012 Ionic current rectification in soft-matter diodes with liquid-metal electrodes *Adv. Funct. Mater.* **22** 625–31

[107] Koo H, So J, Dickey M D and Velev O D 2011 Towards all-soft matter circuits: prototypes of quasi-liquid devices with memristor characteristics *Adv. Mater.* **23** 3559–64

[108] Park Y, Majidi C, Kramer R, Berard P and Wood R J 2010 Hyperelastic pressure sensing with a liquid-embedded elastomer *J. Micromech. Microeng.* **20** 125029

[109] Park Y L, Chen B R and Wood R J 2012 Design and fabrication of soft artificial skin using embedded microchannels and liquid conductors *IEEE Sensors J.* **12** 2711–8

[110] Park Y, Chen B and Wood R J 2011 Soft artificial skin with multi-modal sensing capability using embedded liquid conductors *2011 IEEE Sensors (Limerick, Ireland)* pp 81–4

[111] Ponce Wong R D, Posner J D and Santos V J 2012 Flexible microfluidic normal force sensor skin for tactile feedback *Sensors Actuators* A **179** 62–9

[112] Kramer R K, Majidi C and Wood R J 2011 Wearable tactile keypad with stretchable artificial skin *IEEE Int. Conf. on Robotics and Automation (Shanghai, China)* pp 1103–7

[113] Cheng S and Wu Z 2011 A microfluidic, reversibly stretchable, large-area wireless strain sensor *Adv. Funct. Mater.* **21** 2282–90

[114] Majidi C, Kramer R and Wood R J 2011 A non-differential elastomer curvature sensor for softer-than-skin electronics *Smart Mater. Struct.* **20** 105017

[115] Kramer R K, Majidi C, Sahai R and Wood R J 2011 Soft curvature sensors for joint angle proprioception *IEEE/RSJ Int. Conf. on Intelligent Robots and Systems (San Francisco CA, USA)* pp 1919–26

[116] Zhu S, So J, Mays R, Desai S, Barnes W R, Pourdeyhimi B and Dickey M D 2013 Ultrastretchable fibers with metallic conductivity using a liquid metal alloy core *Adv. Funct. Mater.* **23** 2308–14

[117] Mineart K P, Lin Y, Desai S C, Krishnan A S, Spontak R J and Dickey M D 2013 Ultrastretchable, cyclable and recyclable 1- and 2-dimensional conductors based on physically cross-linked thermoplastic elastomer gels *Soft Matter* **9** 7695–700

[118] Cheng S, Rydberg A, Hjort K and Wu Z 2009 Liquid metal stretchable unbalanced loop antenna *Appl. Phys. Lett.* **94** 144103

[119] Cumby B L, Hayes G J, Dickey M D, Justice R S, Tabor C E and Heikenfeld J C 2012 Reconfigurable liquid metal circuits by Laplace pressure shaping *Appl. Phys. Lett.* **101** 174102

[120] Jeong S H, Hjort K and Wu Z 2015 Tape transfer atomization patterning of liquid alloys for microfluidic stretchable wireless power transfer *Sci. Rep.* **5** 8419

[121] Hrehorova E, Rebros M, Pekarovicova A, Bazuin B, Ranganathan A, Garner S, Merz G, Tosch J and Boudreau R 2011 Gravure printing of conductive inks on glass substrates for applications in printed electronics *J. Display Technol.* **7** 318–24

[122] Gravure Association of America and Gravure Education Foundation 1991 *Gravure: Process and Technology* (Rochester, NY: Gravure Association of America) p 462

[123] Jeong S H, Hjort K and Wu Z 2014 Tape transfer printing of a liquid metal alloy for stretchable RF electronics *Sensors* **14** 16311

[124] Sen P and Kim C-J 2009 Microscale liquid-metal switches—a review *IEEE Trans. Ind. Electron.* **56** 1314–30

[125] Zheng Y, Zhang Q and Liu J 2013 Pervasive liquid metal based direct writing electronics with roller-ball pen *AIP Adv.* **3** 112117

[126] Gao Y, Li H and Liu J 2012 Direct writing of flexible electronics through room temperature liquid metal ink *PloS One* **7** e45485

[127] Gao Y, Li H and Liu J 2013 Directly writing resistor, inductor and capacitor to composite functional circuits: a super-simple way for alternative electronics *PloS One* **8** e69761

[128] Yang J and Liu J 2014 Direct printing and assembly of FM radio at the user end via liquid metal printernull *Circuit World* **40** 134–40

[129] Wang Q, Yu Y, Yang J and Liu J 2015 Fast fabrication of flexible functional circuits based on liquid metal dual-trans printing *Adv. Mater.* **27** 7109–16

[130] Zheng Y, He Z, Gao Y and Liu J 2013 Direct desktop printed-circuits-on-paper flexible electronics *Sci. Rep.* **3** 1786

[131] Li G, Wu X and Lee D 2016 A galinstan-based inkjet printing system for highly stretchable electronics with self-healing capability *Lab Chip* **16** 1366–73

[132] Boley J W, White E L and Kramer R K 2015 Mechanically sintered gallium–indium nanoparticles *Adv. Mater.* **27** 2355–60

[133] White E L, Case J C and Kramer R K 2016 Multi-element strain gauge modules for soft sensory skins *IEEE. Sensors J.* **16** 2607–16

[134] Siegel A C, Bruzewicz D A, Weibel D B and Whitesides G M 2007 Microsolidics: fabrication of three-dimensional metallic microstructures in poly(dimethylsiloxane) *Adv. Mater.* **19** 727–33

[135] Pourbaix M 1974 *Atlas of Electrochemical Equilibria in Aqueous Solutions* (Houston, TX: National Association of Corrosion Engineers)

[136] Dickey M D 2014 Emerging applications of liquid metals featuring surface oxides *ACS Appl. Mater. Interfaces* **6** 18369–79

[137] Zuckerman J J and Hagen A P 2007 *Inorganic Reactions and Methods* (New York: Wiley)

[138] Kim D, Thissen P, Viner G, Lee D, Choi W, Chabal Y J and Lee J 2013 Recovery of nonwetting characteristics by surface modification of gallium-based liquid metal droplets using hydrochloric acid vapor *ACS Appl. Mater. Interfaces* **5** 179–85

[139] Kim D, Lee Y, Lee D, Choi W and Lee J 2013 Hydrochloric acid-impregnated paper for liquid metal microfluidics *IEEE Transducers & Eurosensors: Proc. 17th Int. Conf. on Solid-State Sensors, Actuators and Microsystems (Barcelona, Spain)* pp 2620–3

[140] Wang J, Liu S, Guruswamy S and Nahata A 2013 Reconfigurable liquid metal based terahertz metamaterials via selective erasure and refilling to the unit cell level *Appl. Phys. Lett.* **103** 221116

[141] Li G, Parmar M and Lee D 2015 An oxidized liquid metal-based microfluidic platform for tunable electronic device applications *Lab Chip* **15** 766–75

[142] Dezellus O and Eustathopoulos N 2010 Fundamental issues of reactive wetting by liquid metals *J. Mater. Sci.* **45** 4256–64

[143] Kramer R K, Boley J W, Stone H A, Weaver J C and Wood R J 2014 Effect of microtextured surface topography on the wetting behavior of eutectic gallium–indium alloys *Langmuir* **30** 533–9

[144] Bico J, Thiele U and Quere D 2002 Wetting of textured surfaces *Colloids Surf. Physicochem. Eng. Aspects* **206** 41–6

[145] Kim D, Lee D W, Choi W and Lee J B 2013 A super-lyophobic 3D PDMS channel as a novel microfluidic platform to manipulate oxidized galinstan *J. Microelectromech. Syst.* **22** 1267–75

[146] Kim D, Jung D, Yoo J H, Lee Y, Choi W, Lee G S, Yoo K and Lee J B 2014 Stretchable and bendable carbon nanotube on PDMS super-lyophobic sheet for liquid metal manipulation *J. Micromech. Microeng.* **24** 055018

[147] Jung Y C and Bhushan B 2009 Mechanically durable carbon nanotube-composite hierarchical structures with superhydrophobicity, self-cleaning, and low-drag *ACS Nano* **3** 4155–63

[148] Lau K K S, Bico J, Teo K B K, Chhowalla M, Amaratunga G A J, Milne W I, McKinley G H and Gleason K K 2003 Superhydrophobic carbon nanotube forests *Nano Lett.* **3** 1701–5

[149] Bayer I S, Steele A and Loth E 2013 Superhydrophobic and electroconductive carbon nanotube-fluorinated acrylic copolymer nanocomposites from emulsions *Chem. Eng. J.* **221** 522–30

[150] Li H, Wang X, Song Y, Liu Y, Li Q, Jiang L and Zhu D 2001 Super-'amphiphobic' aligned carbon nanotube films *Angew. Chem. Int. Ed.* **40** 1743–6

[151] Madou M J 2011 *Fundamentals of Microfabrication and Nanotechnology* 3rd edn (Boca Raton, FL: CRC Press)

[152] Mack C 2007 *Fundamental Principles of Optical Lithography: The Science of Microfabrication* (New York: Wiley)

[153] Gao Y and Bando Y 2002 Nanotechnology: carbon nanothermometer containing gallium *Nature* **415** 599–600

[154] Liu Z, Bando Y, Mitome M and Zhan J 2004 Unusual freezing and melting of gallium encapsulated in carbon nanotubes *Phys. Rev. Lett.* **93** 095504

[155] Wang L and Liu J 2014 Liquid phase 3D printing for quickly manufacturing conductive metal objects with low melting point alloy ink *Sci. China Technol. Sci.* **57** 1721–8

[156] Wang L and Liu J 2014 Compatible hybrid 3D printing of metal and nonmetal inks for direct manufacture of end functional devices *Sci. China Technol. Sci.* **57** 2089–95

[157] Gross F B 2011 *Frontiers in Antennas: Next Generation Design & Engineering* (New York: McGraw-Hill)

[158] Ohta A T, Guo S, Lei B J, Hu W and Shiroma W A 2012 A liquid-metal tunable electromagnetic-bandgap microstrip filter *IEEE Int. Conf. on Wireless Information Technology and Systems (Maui, Hawaii, USA)* pp 1–4

[159] Khan M R, Hayes G J, Zhang S, Dickey M D and Lazzi G 2012 A pressure responsive fluidic microstrip open stub resonator using a liquid metal alloy *IEEE Microw. Compon. Lett.* **22** 577–9

[160] Chen C and Peroulis D 2007 Liquid RF MEMS wideband reflective and absorptive switches *IEEE Trans. Microw. Theory Technol.* **55** 2919–29

[161] Li M and Nader B 2012 Fluidically tunable frequency selective/phase shifting surfaces for high-power microwave applications *IEEE Trans. Antennas Propag.* **60** 2748–59

[162] Morishita A M, Kitamura C K Y, Ohta A T and Shiroma W A 2013 A liquid-metal monopole array with tunable frequency, gain, and beam steering *IEEE Antennas Wireless Propag. Lett.* **12** 1388–91

[163] Dey A, Guldiken R and Mumcu G 2013 Wideband frequency tunable liquid metal monopole antenna *IEEE Int. Symposium on Antennas and Propagation Society (Orlando, Florida, USA)* pp 392–3

[164] Kim D, Pierce R G, Henderson R, Doo S J, Yoo K and Lee J 2014 Liquid metal actuation-based reversible frequency tunable monopole antenna *Appl. Phys. Lett.* **105** 234104

[165] Khan M R, Hayes G J, So J, Lazzi G and Dickey M D 2011 A frequency shifting liquid metal antenna with pressure responsiveness *Appl. Phys. Lett.* **99** 013501

[166] Hayes G J, So J, Qusba A, Dickey M D and Lazzi G 2012 Flexible liquid metal alloy (EGaIn) microstrip patch antenna *IEEE Trans. Antennas Propag.* **60** 2151–6

[167] Wang J, Liu S and Nahata A 2012 Reconfigurable plasmonic devices using liquid metals *Opt. Express* **20** 12119–26

[168] Wang M, Trlica C, Khan M R, Dickey M D and Adams J J 2015 A reconfigurable liquid metal antenna driven by electrochemically controlled capillarity *J. Appl. Phys.* **117** 194901

[169] Li G, Parmar M, Kim D, Lee J B and Lee D 2014 PDMS based coplanar microfluidic channels for the surface reduction of oxidized Galinstan *Lab Chip* **14** 200–9

[170] Kim D, Lee D, Choi W and Lee J 2012 A super-lyophobic PDMS micro-tunnel as a novel microfluidic platform for oxidized Galinstan® *IEEE 25th Int. Conf. on Micro Electro Mechanical Systems (Paris, France)* pp 1005–8

[171] Hutter T, Bauer W C, Elliott S R and Huck W T S 2012 Formation of spherical and non-spherical eutectic gallium–indium liquid-metal microdroplets in microfluidic channels at room temperature *Adv. Funct. Mater.* **22** 2624–31

[172] Koo C, LeBlanc B E, Kelley M, Fitzgerald H E, Huff G H and Han A 2015 Manipulating liquid metal droplets in microfluidic channels with minimized skin residues toward

tunable RF applications *J. Microelectromech. Syst.* **24** 1069–76

[173] Khan M R, Trlica C, So J, Valeri M and Dickey M D 2014 Influence of water on the interfacial behavior of gallium liquid metal alloys *ACS Appl. Mater. Interfaces* **6** 22467–73

[174] Gough R C, Morishita A M, Dang J H, Hu W, Shiroma W A and Ohta A T 2014 Continuous electrowetting of non-toxic liquid metal for RF Applications *IEEE Access* **2** 874–82

[175] Tang S, Lin Y, Joshipura I D, Khoshmanesh K and Dickey M D 2015 Steering liquid metal flow in microchannels using low voltages *Lab Chip* **15** 3905–11

[176] Khan M R, Trlica C and Dickey M D 2015 Recapillarity: electrochemically controlled capillary withdrawal of a liquid metal alloy from microchannels *Adv. Funct. Mater.* **25** 671–8

[177] Deng Y G and Liu J 2009 Corrosion development between liquid gallium and four typical metal substrates used in chip cooling device *Appl. Phys.* A **95** 907–15

[178] Diedhiou D L, Sagazan O d, Sauleau R and Boriskin A V 2014 Contactless microstrip transition for flexible microfluidic circuits and antennas *IEEE Antennas Wireless Propag. Lett.* **14** 1502–5

[179] Ahlberg P, Jeong S H, Jiao M, Wu Z, Jansson U, Zhang S-L and Zhang Z-B 2014 Graphene as a diffusion barrier in galinstan-solid metal contacts *IEEE Trans. Electron Dev.* **61** 2996–3000